CR 135328

(NASA-CR-135328) STIFFNESS AND DAMPING OF ELASTOMERIC O-RING BEARING MOUNTS Contractor Report, Sep. 1975 - Jan. 1977 (Mechanical Technology, Inc.) 75 p HC A04/MF A01 CSCL 13I G3/39

N78-19460

Unclas 06930

MTI

MTI

MTI

MTI

MTI

MTI

Mechanical Technology Incorporated

Research and Development Division

78TR17

STIFFNESS AND DAMPING OF ELASTOMERIC O-RING BEARING MOUNTS

Prepared Under
Contract No. NAS 3-19751

Prepared for:
National Aeronautics and Space Administration
Lewis Research Center
November 1977

MECHANICAL TECHNOLOGY INCORPORATED
968 Albany-Shaker Road
Latham, New York 12110

78TR17

STIFFNESS AND DAMPING OF ELASTOMERIC O-RING BEARING MOUNTS

Prepared For:
National Aeronautics and Space Administration
Lewis Research Center

Prepared Under:
Contract No. NAS 3-19751

November 1977

MECHANICAL TECHNOLOGY INCORPORATED
968 Albany-Shaker Road
Latham, New York 12110

1. Report No. CR-135328	2. Government Accession No.	3. Recipient's Catalog No.
4. Title and Subtitle Stiffness and Damping of Elastomeric O-Ring Bearing Mounts		5. Report Date November 1977 6. Performing Organization Code
7. Author(s) A.J. Smalley, M.S. Darlow, R.K. Mehta		8. Performing Organization Report No. MTI 78TR17 10. Work Unit No.
9. Performing Organization Name and Address Mechanical Technology Incorporated 968 Albany-Shaker Road Latham, New York 12110		11. Contract or Grant No. NAS3-19751
12. Sponsoring Agency Name and Address National Aeronautics and Space Administration Washington, D.C. 20546		13. Type of Report and Period Covered Contractor Report September, '75 - January, '77 14. Sponsoring Agency Code

15. Supplementary Notes
"Final Report" Project Manager Zalton N. Nemeth, Fluid System Components Division, National Aeronautics and Space Administration, Lewis Research Center, Cleveland, Ohio

16. Abstract

A test rig to measure the dynamic stiffness and damping of elastomer O-rings is described. Test results for stiffness and loss coefficient in the frequency range from 50 Hz to 1000 Hz are presented. Results are given for three different materials (Viton-70, Viton-90, and Buna N-70), for five temperatures (25°, 38°, 56°, 149°, and 216°C), for three amplitudes (7.62, 25.4, and 127 x 10^{-6}m), for five values of squeeze (5, 10, 15, 20, and 30 percent), for three values of stretch (0, 5, and 10 percent), for three values of cross-section diameter (1/16, 1/8, and 3/16 inch nominal), and for three values of groove width (115, 135, and 150 percent of cross-section diameter). All test data points are plotted. In addition, trend summary plots are presented which compare the effect of material, temperature, amplitude, squeeze, stretch, cross-section diameter, and groove width. O-ring deflections under a static load for different material are presented; and effective static stiffness values are compared with dynamic values.

17. Key Words (Suggested by Author(s))		18. Distribution Statement
Damping	Elastomers	Unlimited
Dampers	Viscoelasticity	
O-rings		
Bearing Mounts		

19. Security Classif. (of this report)	20. Security Classif. (of this page)	21. No. of Pages	22. Price*
Unclassified	Unclassified	76	

*For sale by the National Technical Information Service, Springfield, Virginia 22161

NASA-C-168 (Rev. 10-75)

ABSTRACT

A test rig to measure the dynamic stiffness and damping of elastomer O-rings is described. Test results for stiffness and loss coefficient in the frequency range from 50 Hz to 1000 Hz are presented. Results are given for three different materials (Viton-70, Viton-90, and Buna N-70), for five temperatures (25°, 38°, 56°, 149°, and 216°C), for three amplitudes (7.62, 25.4, and 127 x 10^{-6} m), for five values of squeeze (5, 10, 15, 20, and 30 percent), for three values of stretch (0, 5, and 10 percent), for three values of cross-section diameter (1/16, 1/8, and 3/16 inch nominal), and for three values of groove width (115, 135, and 150 percent of cross-section diameter). All test data points are plotted. In addition, trend summary plots are presented which compare the effect of material, temperature, amplitude, squeeze, stretch, cross-section diameter, and groove width. O-ring deflections under a static load for different material are presented; and effective static stiffness values are compared with dynamic values.

SUMMARY

This report presents an investigation of the dynamic characteristics of flexible bearing mounts in the form of elastomeric O-rings. The previously developed base excitation resonant mass method was used to measure the dynamic stiffness and damping of a pair of O-rings, with nominal outer diameters of 6.35 cm. Test hardware was designed and fabricated to allow controlled variation in imposed squeeze and stretch, in cross-sectional diameter, and in O-ring groove width. In addition, a thermally insulated housing with hot and cold air supplies was designed and fabricated to allow temperatures to be controlled up to 232°C.

A parameter perturbation test program was executed in which each of material, temperature, amplitude, squeeze, stretch, cross-sectional diameter, and groove were varied, in turn, about a nominal value. In all, nineteen combinations of the test parameters were investigated of the some 6075 possible tests.

- Three different materials (Viton-70, Viton-90, Buna N-70)
- Five Temperatures (25°, 38°, 56°, 149°, and 216°C)
- Three amplitudes (7.62, 25.4, 127 x 10^{-6} m)
- Five values of squeeze (5, 10, 15, 20, and 30 percent)
- Three values of stretch (0, 5, and 10 percent)
- Three values of cross-section diameter (1/16, 1/8, and 3/16 inch nominal)
- Three values of groove width (115, 135, and 150 percent of cross-section diameter)

The test data was plotted for each test combination over the full frequency range investigated. These plots are presented in the report in the form of stiffness and loss coefficient versus frequency.

Deflections under a static load were also measured and it is shown in the report that dynamic stiffness values are 4 to 11 times the effective static stiffness. The effect of frequency is particularly pronounced for Viton-70, less so for Viton-90, and least pronounced for Buna N-70. To each set of test data, a power law line is fitted which best represents the experimental variation of stiffness and loss coefficient versus frequency. Using these power

law lines, trend summary plots are created which allow the effect of each test parameter on dynamic O-ring characteristics to be directly assessed. It is shown that stiffness and loss coefficient are weak functions of stretch, groove width, and cross-section diameter. It is further shown that material, squeeze, amplitude, and temperature are significant parameters in the determination of dynamic stiffness and loss coefficient. Increasing squeeze increases stiffness and reduces loss coefficient; increasing amplitude decreases both stiffness and loss coefficient; increasing temperature also reduces both stiffness and loss coefficient.

TABLE OF CONTENTS

LIST OF FIGURES

LIST OF FIGURES (Cont'd)

LIST OF TABLES

1. INTRODUCTION

The use of support damping as a means to control rotationally excited vibrations is seeing increasingly wide application in advanced turbo-machinery. It will also have an important role to play in advanced flexible power transmission shafting. Presently, the most common form of damper in these applications is the squeeze film damper in parallel with some type of mechanical flexure.

Elastomer dampers are an attractive alternative to the squeeze film for rotating machinery and for other applications, because of their simplicity, their inherent combination of stiffness and damping, their compactness, and their lack of need for seals or oil supply. In the form of O-rings or cartridges, they are being considered for low cost engine applications and for helicopter transmission shafting. Two factors which resist the growth and application of elastomer dampers are a limited availability of designer oriented data on their dynamic behavior and limited quantification of problems to be encountered in their application. Dynamic testing under controlled conditions, coupled with effective interpretation of the test results, will help to fill this need. Thereby, the influence of important geometrical, environmental and material parameters can be determined.

This report presents results of a study to determine the stiffness and damping characteristics of elastomeric O-rings. These characteristics have been determined as a function of frequency. The effects of the following test parameters have been investigated.

TABLE 1

O-RING PARAMETERS INVESTIGATED

Material	Squeeze
Cross-Section Diameter	Stretch
Temperature	Groove Width
Amplitude	(Frequency)

The base excitation resonant mass method (1) has been used in conjunction with a computerized system for data acquisition and data reduction. Generally, consistent data has been obtained and the trends resulting from the parameter changes are qualitatively as would be expected. Worthy of particular mention are the pronounced effects of temperature and vibration amplitude in decreasing stiffness and damping.

The test program resulted in a substantial volume of data which is presented in the report in full, in the form of measured stiffness and loss coefficient as a function of frequency for each test condition. The effects of each test parameter are then summarized in the form of trend summary plots in which parallel fits to the data for each test condition are compared on one frame for each test parameter. Finally cross-plots emphasizing the major trends exhibited by the test results are presented.

The data in this report can be effectively used to design and predict performance of a Viton-70 O-ring flexible bearing mount. Good guidance can also be obtained in the design of Viton-90 and Buna N mounts. For other materials, the results are expected to be typical, but it is recommended that confirmatory performance tests be undertaken.

2. TEST RIG DESIGN

The objectives of the test rig design were to provide the ability to determine stiffness and damping of O-rings acting as radial bearing mounts. The target frequency range was 20 to 1000 Hz. The low amplitude goal was 0.3 mils (7.62×10^{-6}m) across the elastomer. The high amplitude goal was 5 mils at frequencies up to 600 Hz, decreasing in inverse proportion to frequency between 600 and 1000 Hz. The temperature objectives were to be able to control temperatures between 25°C (77°F) and 232°C (450°F). These goals are summarized in Table 2. The O-ring diameter was to be 2-1/2 inches, and capability to vary squeeze, stretch, O-ring cross-section, groove width, and material were to be provided.

TABLE 2

TEST RIG OBJECTIVES

Temperature	25°C to 232°C (77°F to 450°F)	
Amplitude	7.62×10^{-6} to 1.27×10^{-4} m	(0.3 to 5 mils)
Frequency	20 to 1000 Hz	

After an assessment of feasibility the previously developed base excitation resonant mass method (1) was selected. This test method, as applied to O-ring flexible mounts, is illustrated schematically in Figure 1. In summary, the test method employs a pair of O-rings to support a mass on an electromagnetic shake table so that the mass and O-rings form a one degree of freedom damped system for vertical motion. When the table is shaken near the resonant frequency of the ring-mass system, the relative motion across the ring is an amplification of the table motion and there is a phase shift across the elastomer of the order of 90°. The critical sensors for the test method are accelerometers mounted on the table and on the resonant mass. From the amplitude ratio and phase angle between the accelerometer signals, at a particular frequency, and from the known value of supported mass, the stiffness and damping are inferred. The test method and data reduction equations are described in References [1], [2], [3], and [4].

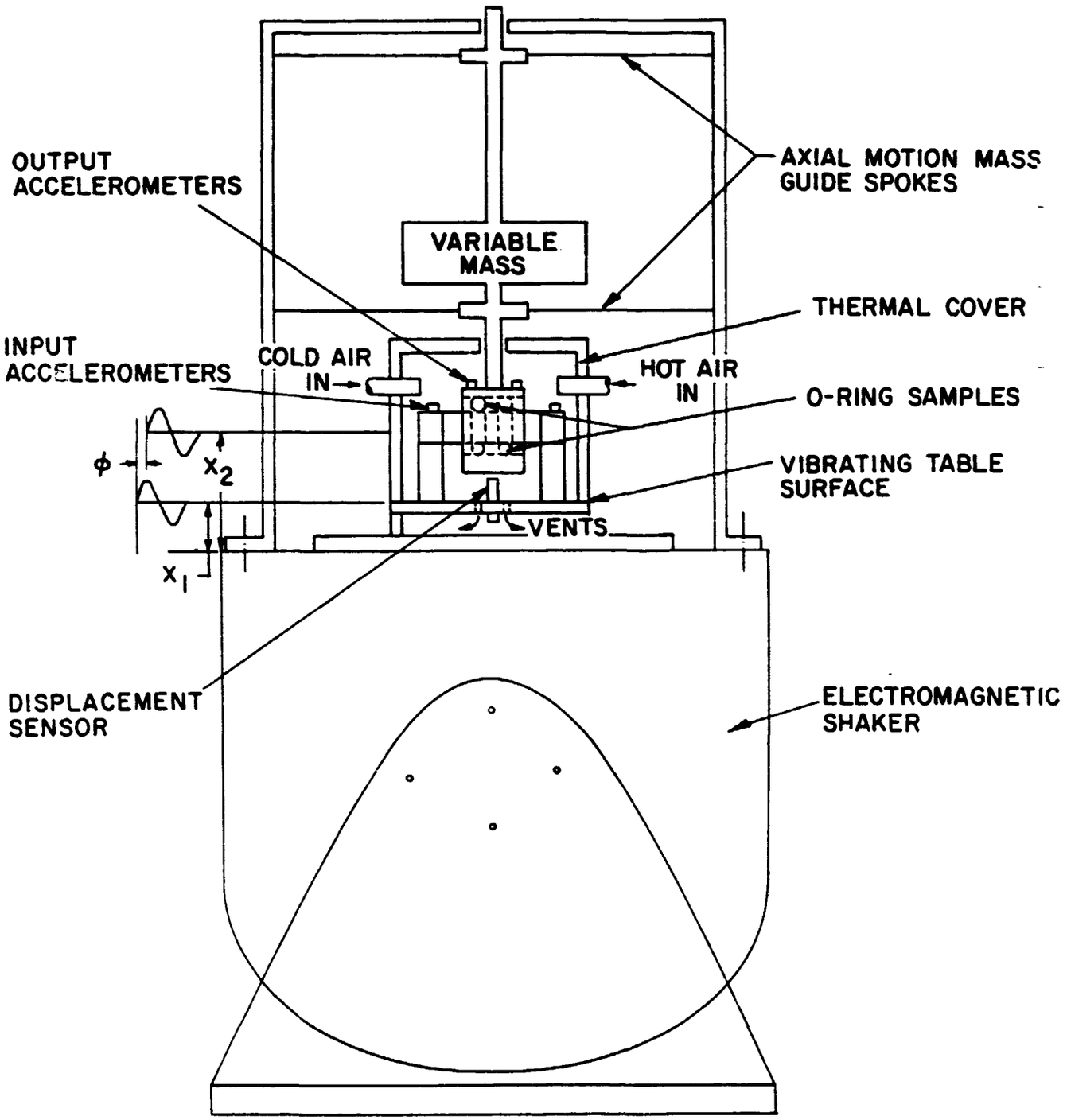

Fig. 1 Schematic of Base Excitation, Resonant Mass Test Rig for O-Ring Investigations

Using estimated values for O-ring stiffness, a range of supported masses between one-half pound and three hundred pounds would cover the frequency range between 20 Hz and 1000 Hz with resonant or near resonant operation. At the practical limit of the shaker table (80 G's at 600 Hz), a table double amplitude of 1.1 x 10^{-4} meters is possible and relatively small resonant amplification factor would be needed to meet the goal of 1.27 x 10^{-4} meters across the elastomer. Temperature objectives were to be achieved by means of a well insulated thermal cover and insulated base to enclose the test specimen. High temperature heating air together with controllable cooling air were provided to accurately control the temperature.

The relative dimensions and arrangement of the test rig can be seen in the assembly drawing of Figure 2. Figure 3 is a view of the test rig parts prior to assembly. It shows two O-rings (of different cross-sectional diameters). For all tests the rings were seated in grooves cut in a sleeve (2) which could be replaced with a similar part to change inner diameter and groove width as required by the test schedule. This sleeve was mounted on a non-rotating "shaft" (3) with slight interference fits at two different diameters: an arrangement which led to simple assembly and disassembly by means of extractor screws. The shaft was bolted to two mounting blocks which were themselves attached to an insulated base plate (4). Supported on the rings for most tests was a 1.26 kg housing (5). This housing was replaced with a similar part to change inner diameter as required by the test schedule. To the 1.26 kg housing an extension could be attached into which a vertical rod carrying a loading platform could be screwed to achieve higher supported masses. For high frequency tests, with "soft" O-ring configurations, a light (0.21 kg) shell housing replaced the 1.26 kg housing. The base plate was mounted on the shaker table on eight spacers (9). Also shown in Figure 3 is the insulated thermal cover for high temperature tests.

The photographs in Figures 4 through 8 provide various views of the test rig at different stages of assembly. In Figure 4 the thermal housing is shown together with the 1.26 kg housing mounted on the shaft. Figure 5 is a photograph of the test rig with 1.26 kg housing shown, from an angle, mounted on the shaker. In Figure 6 a similar side view is shown. In Figure 7 the 1.26 kg housing is seen replaced by the 0.21 kg shell mass. In Figure 8 an overall view of the assembled rig is seen with the thermal cover in place, and the tri-pod assembly used to laterally stabilize supported masses.

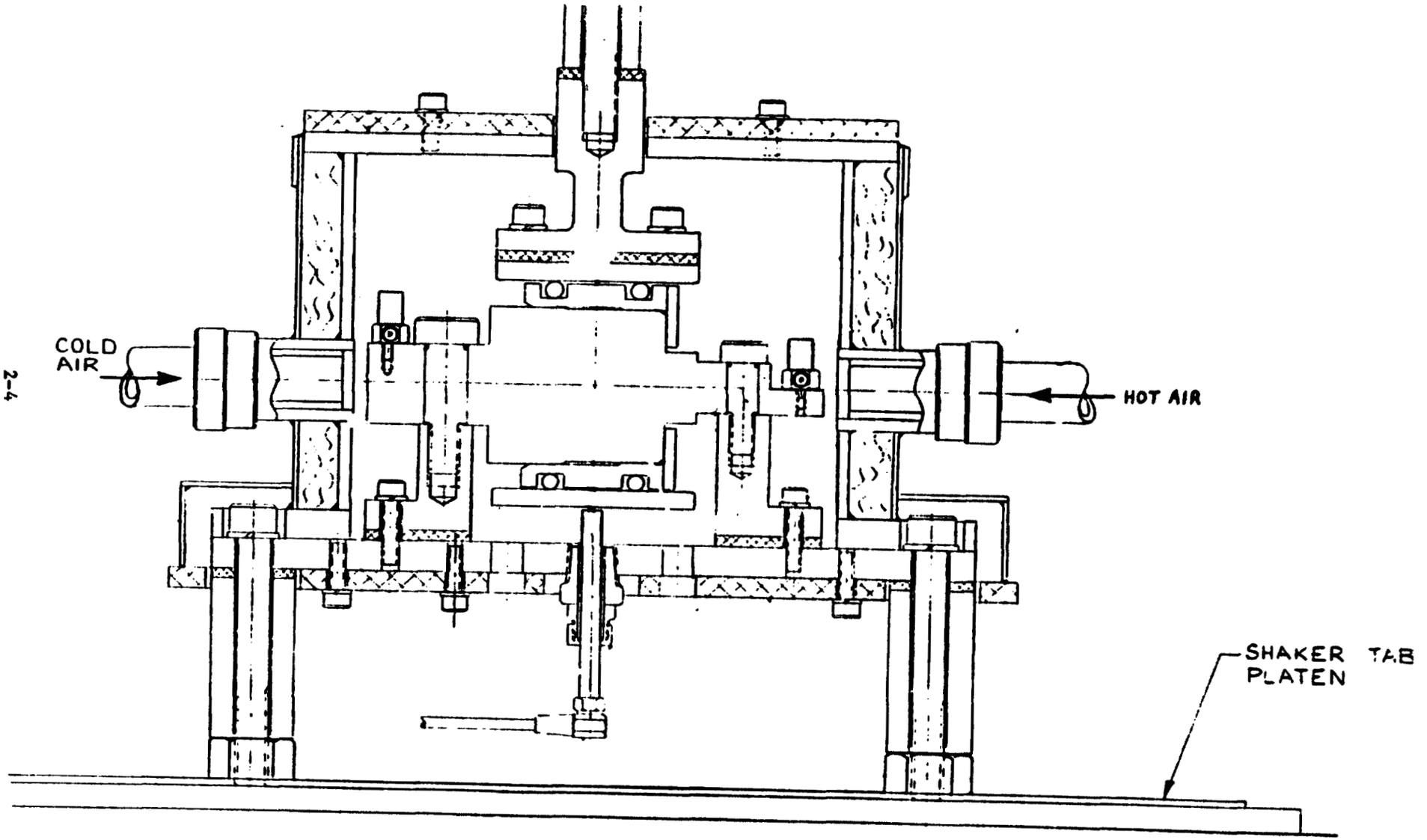

Fig. 2 Assembly Drawing: O-Ring Test Rig

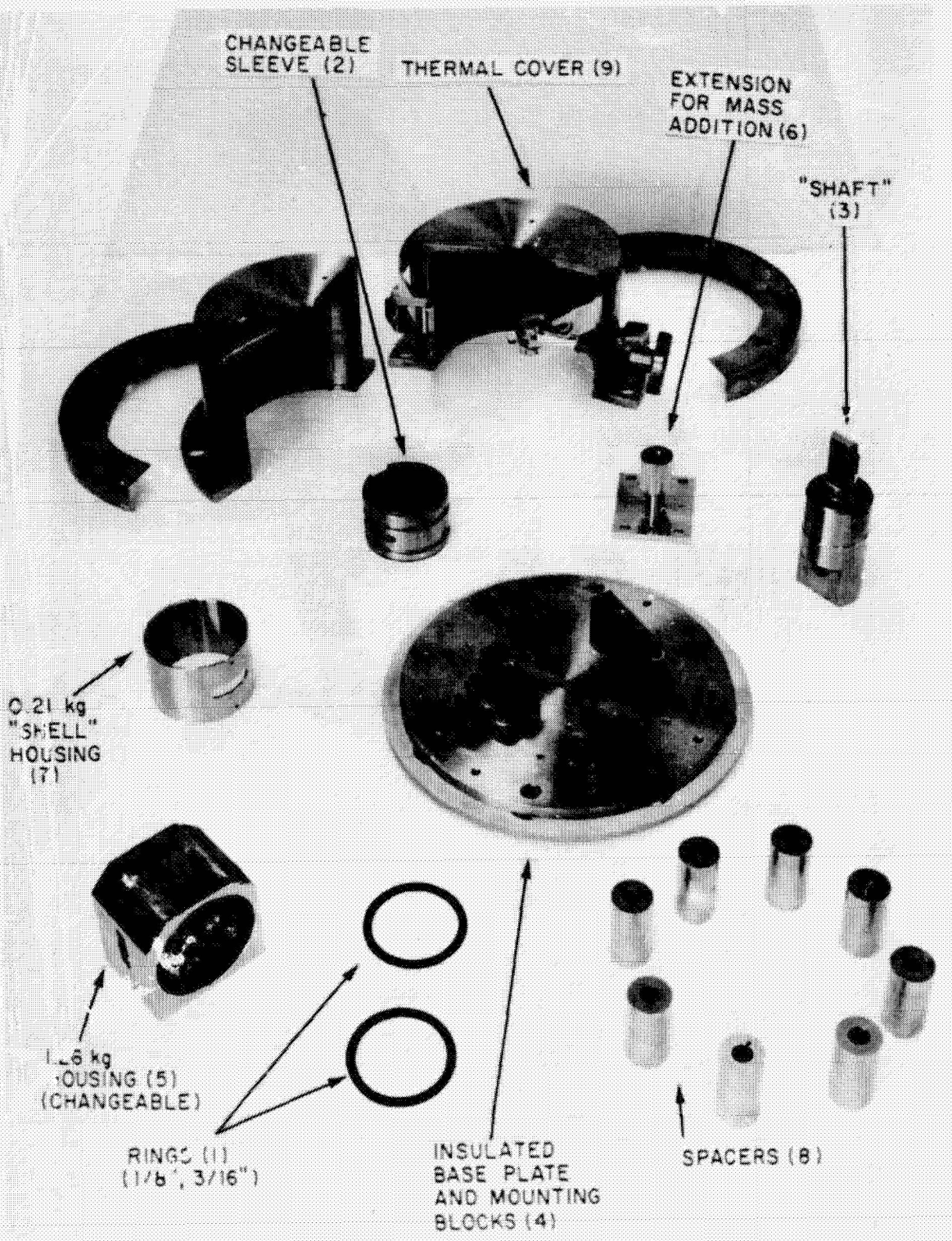

Fig. 3 Test Rig Components

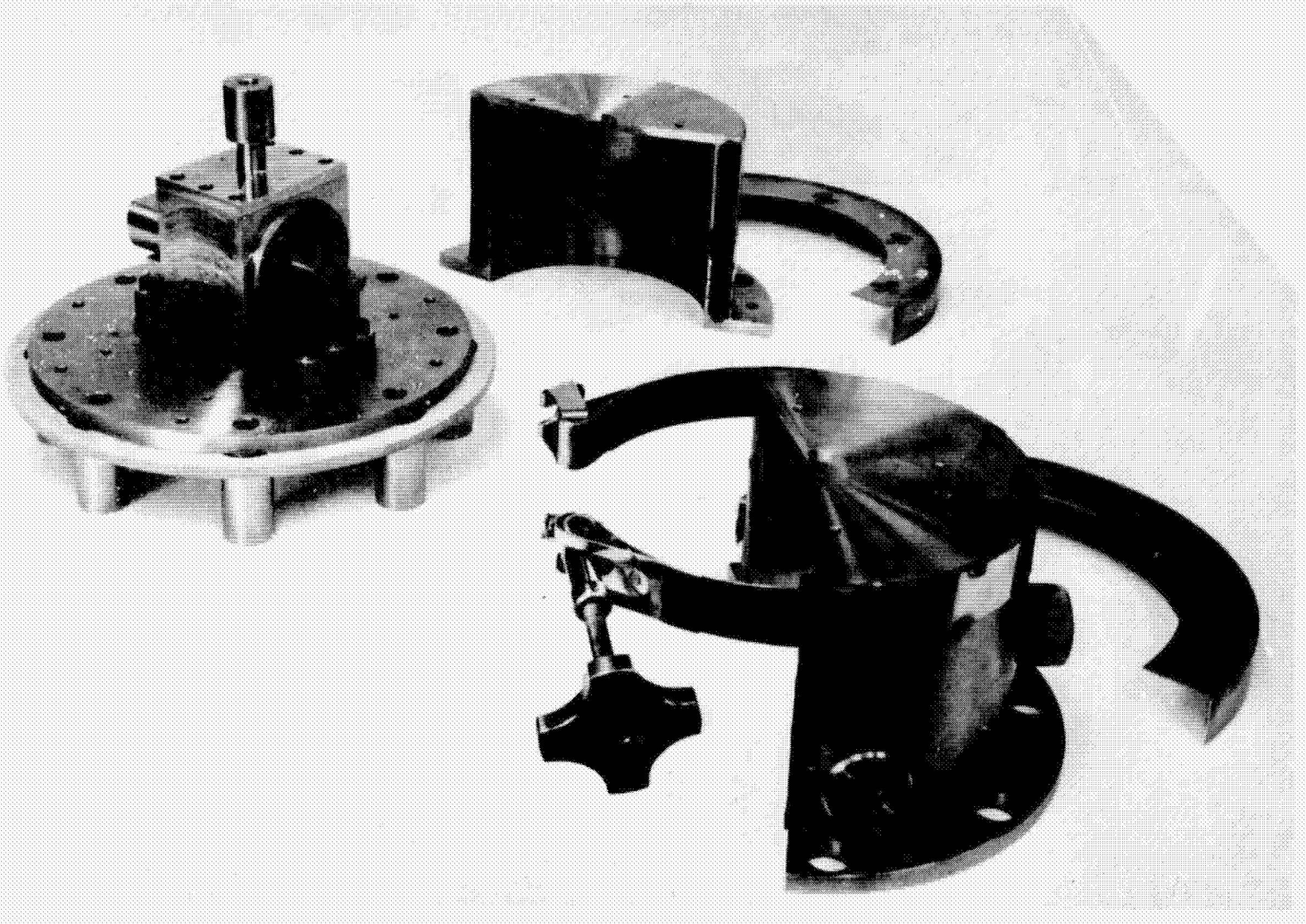

Fig. 4 Partially Assembled Test Rig

MTI-17596

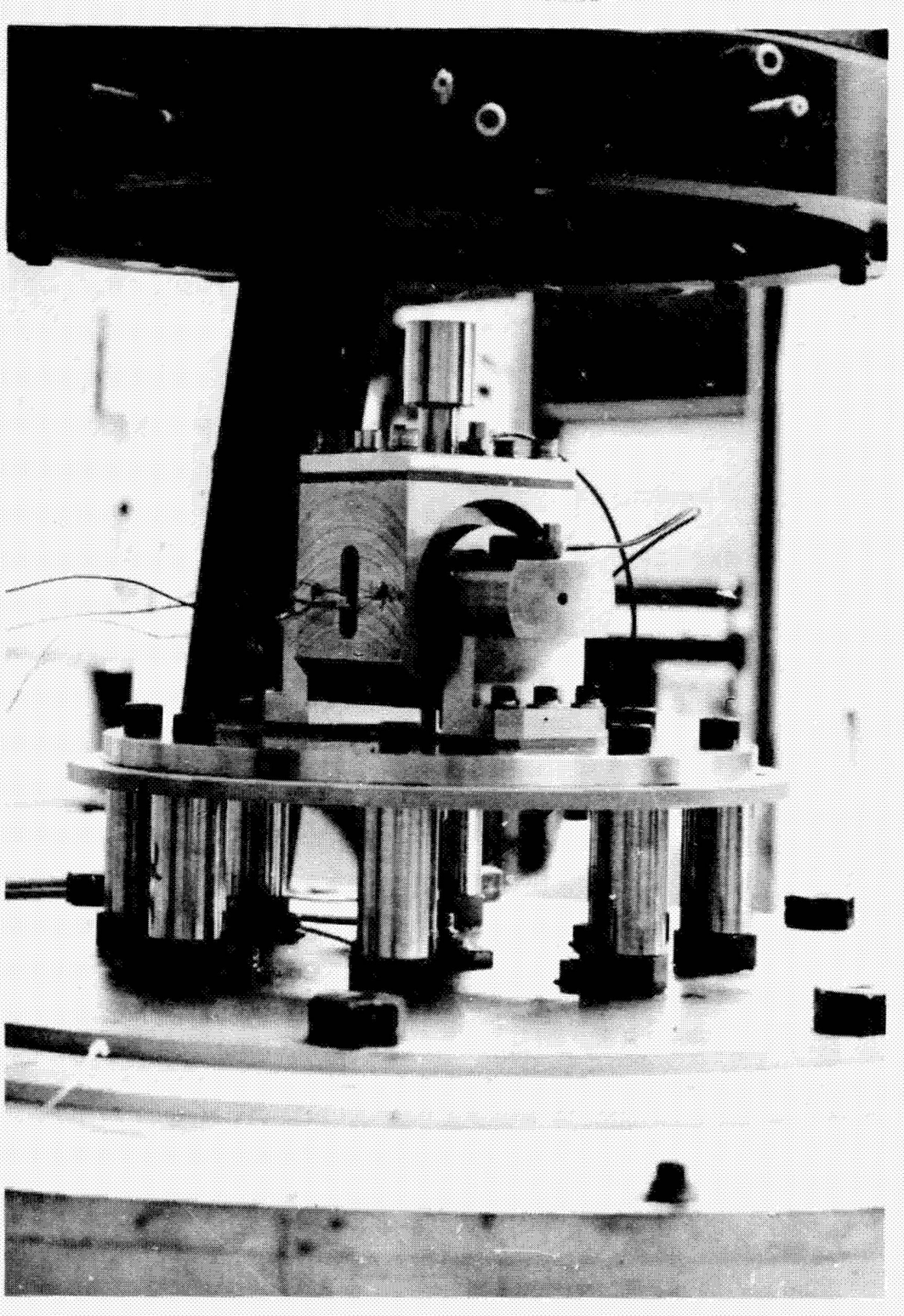

Fig. 5 Test Rig on Shaker - Regular Housing, Diagonal View

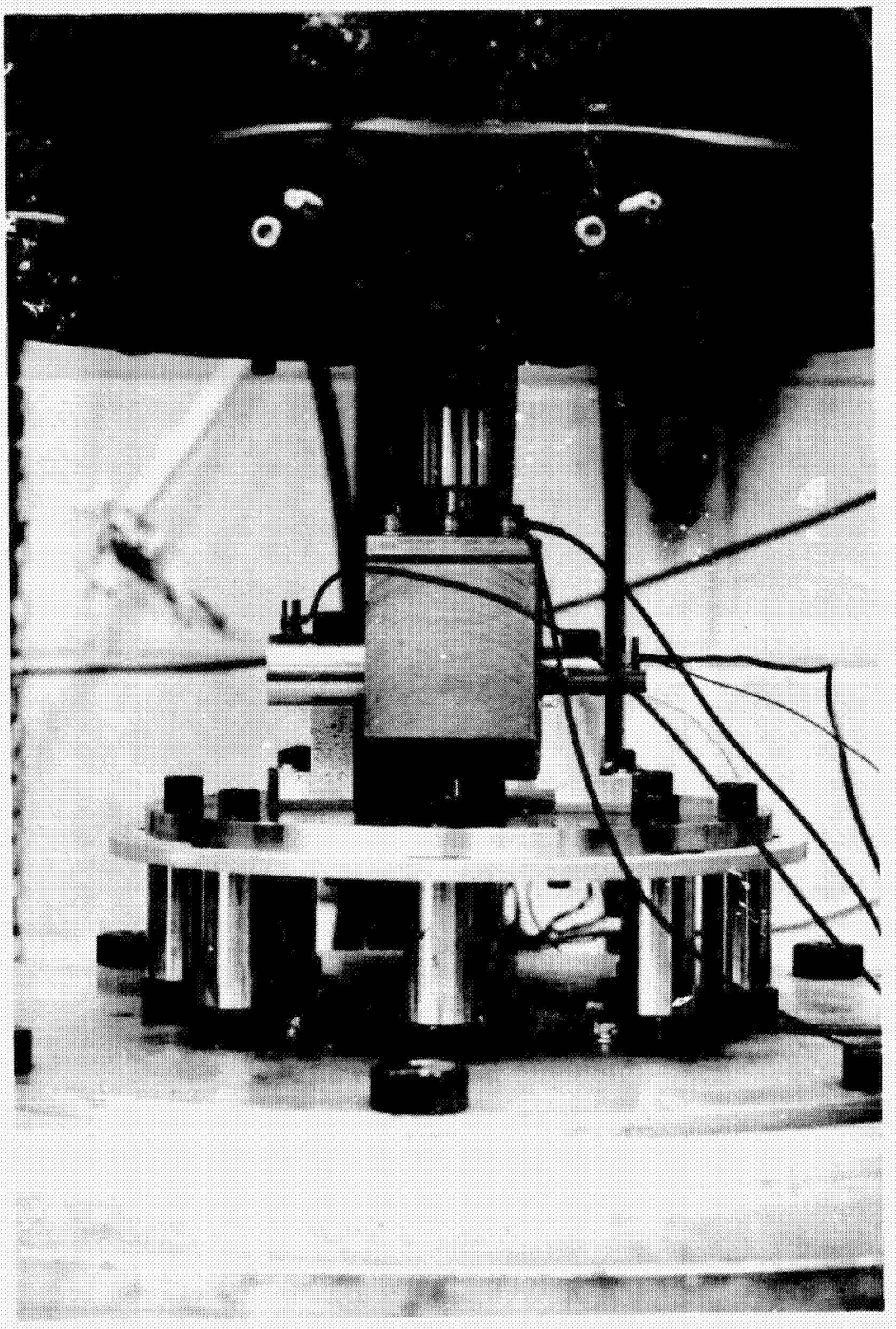

Fig. 6 Test Rig on Shaker - Regular Housing, Side View

MTI-17597

Fig. 7 Test Rig on Shaker - Shell Mass

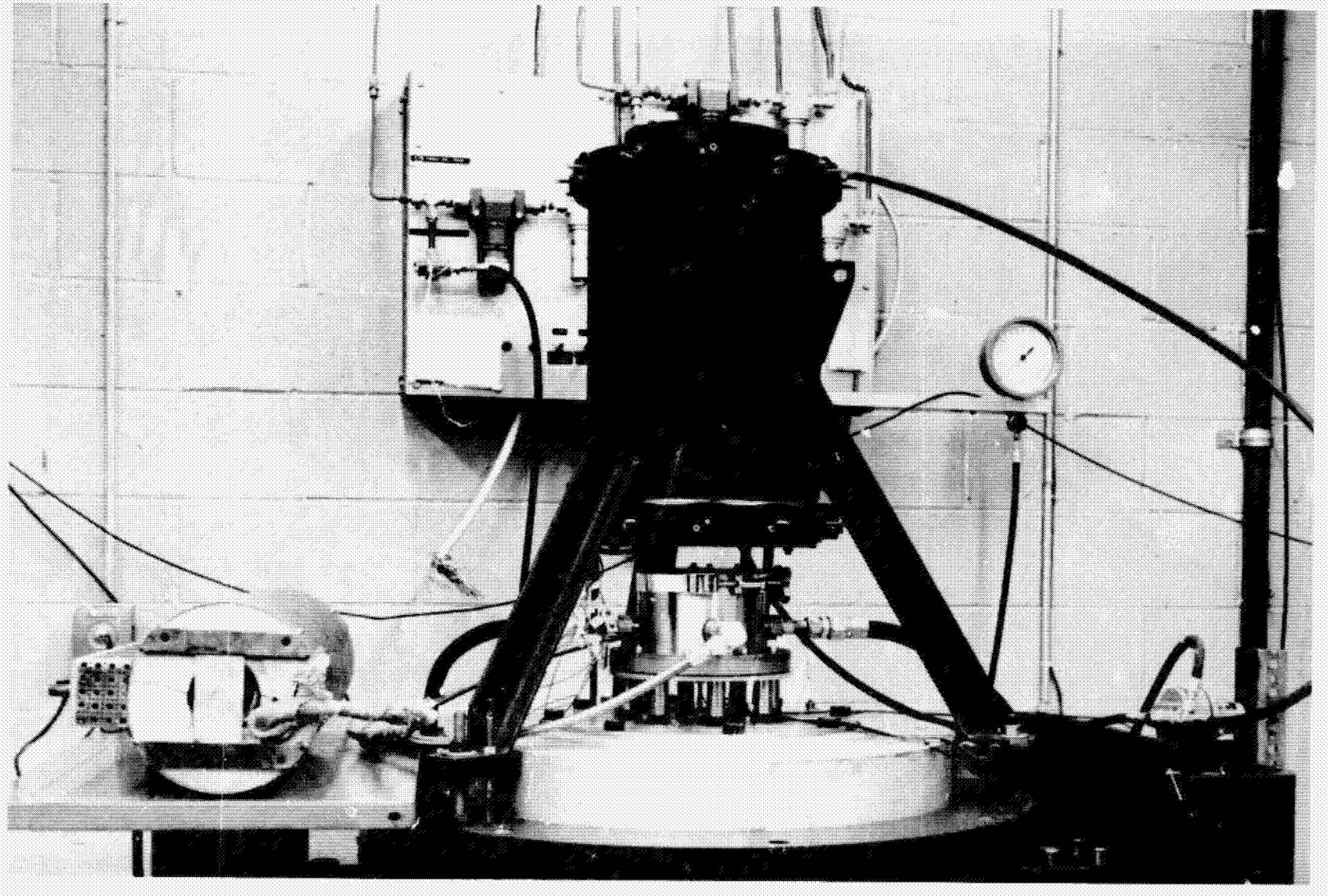

Fig. 8 Test Rig on Shaker Showing Thermal Cover and Tripod

MTI-17599

Test Materials

Batches of the different O-ring material and size combinations were required. In each case the supplier provided documentation that O-rings of one material were made from the same raw material mix. Fifty of each combination of material and cross-section diameter were obtained. Upon receipt of the O-rings, they were inspected to check inner diameter and cross-sectional diameter so that exact dimensions (within approximately 1 mil) could be used in calculations of stretch and squeeze. To check I.D., a shaft made with a series of successively smaller diameter steps was used. O-rings were dropped over this stepped shaft and the point at which they "hung up" gave the inner diameter. The cross-sectional diameter was carefully measured with a micrometer.

Instrumentation

Three sensor types were used in the test rig. Accelerometers were used to measure input and output acceleration - that is acceleration of the shaker table and acceleration of the supported mass. A capacitance probe was used to measure relative displacement across the O-rings and thermocouples were used to measure temperature. The accelerometers were B. and K. high-temperature accelerometers (Model No. 4344). The displacement probe was a ten mil MTI capacitance probe.

Data Acquisition

For all vibration tests, data was acquired by means of a computer controlled data acquisition system, consisting of a dual channel tracking filter, digital voltmeter for amplitude, a phase meter, a multi-channel scanner, a PDP-11/34 minicomputer, and a teletype terminal. Amplitude and phase signals from each accelerometer and from the displacement sensor were captured by the system together with frequency. The finally accepted data point from each channel was the average of ten successive samples. Temperatures from thermocouples at various locations in the test rig were demanded by the computer at various times in the data acquisition process and were entered by hand. Figure 9 provides a schematic of the data acquisition system and its interface with the computer.

Test Procedure

The test procedure for each test assembly was as follows:

1. Operator enters information describing the test conditions and supported mass via the teletype terminal.

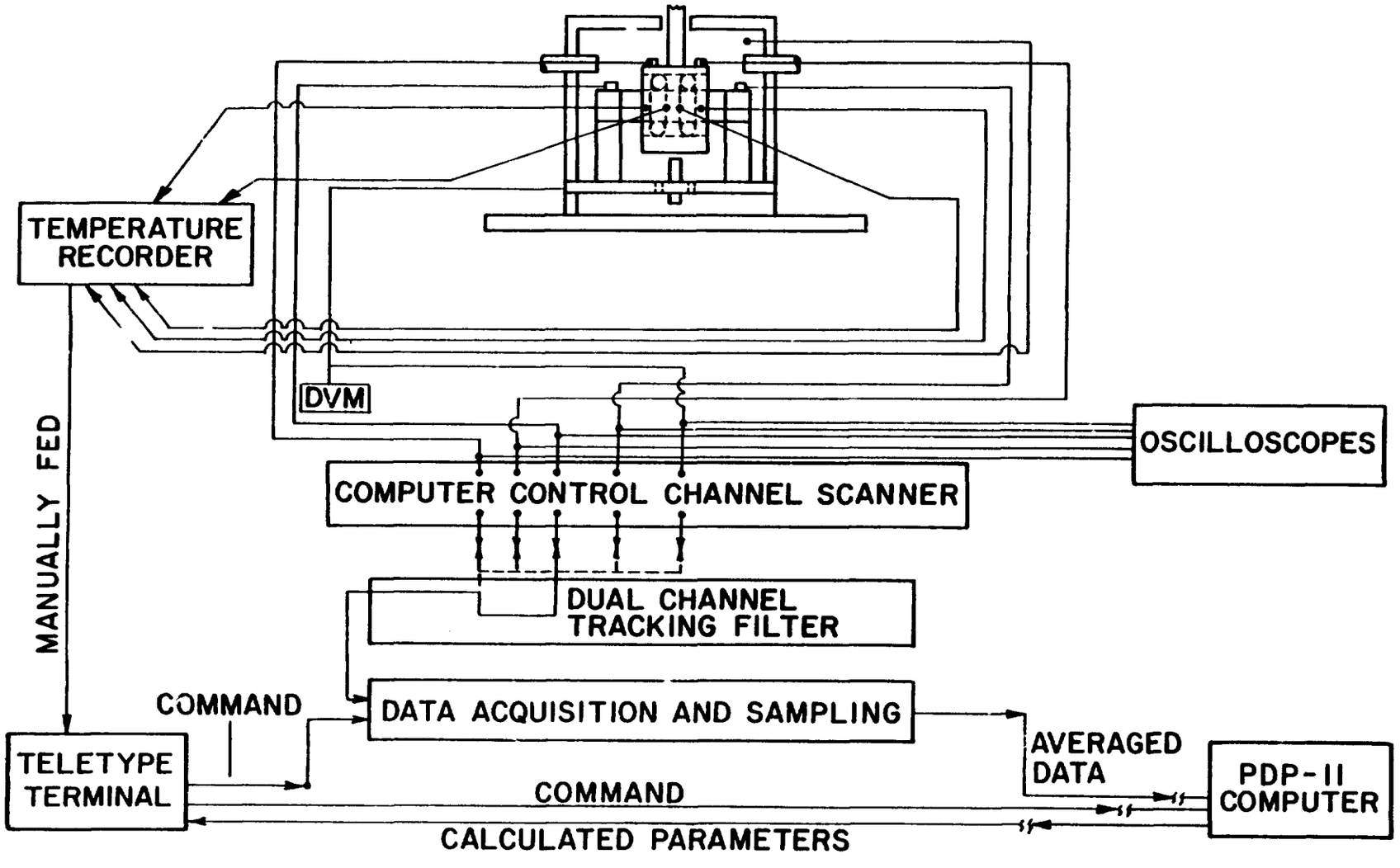

Fig. 9 Data Acquisition Schematic

2. Operator sets shaker at a frequency which gives a 15 degree phase angle (the lowest phase angle at which acceptable data could be obtained).

3. Operator adjusts shaker amplitude until the required amplitude across the O-ring is displayed.

4. Operator checks that the ambient and metal temperature are within two or three degrees of the required temperature condition. If not, hot or cold air flows are adjusted as necessary to bring temperatures into line.

5. Operator instructs computer to acquire data via teletype [illegible].

6. Computer acquires data in the form of amplitude and phase for each sensor and provides an immediate calculation of stiffness and damping. Operator reviews sensor readings and stiffness and damping results, and indicates to the computer either that the data point is acceptable or not acceptable (normally it is acceptable).

7. If acceptable, the computer stores the data on a disk file. If not acceptable, the data point is discarded.

8. Operator selects new frequency to give phase angle 15 degrees higher than previous data point.

9. Steps 2 through 8 are repeated until 165 degree phase angle is reached (the highest at which acceptable data could be obtained).

10. Resonant mass is changed and steps 1 through 9 are repeated for all masses of interest.

This test procedure was followed for each combination of test parameters. As will be discussed in subsequent report sections, 19 different test conditions were investigated to determine the influence of the seven test parameters of interest.

The complexity of a change in test conditions was a function of the parameter being changed, as summarized in Table 3. Most readily changed was amplitude since this simply required altering the shaker control settings. A change in

TABLE 3

ACTIONS NECESSARY TO CHANGE TEST PARAMETERS

To Change	Action
Temperature	Close thermal cover, introduce hot air; and monitor temperatures sensors, adjusting with cold air if necessary.
Amplitude	Adjust shaker amplitude until digital display of displacement sensor amplitude reads required value.
O-Ring Cross-Sectional Diameter	Replace inner sleeve, housing, and O-rings with components of appropriate diameter to give required combination of squeeze and stretch.
Squeeze*	Replace housing with housing of different inner diameter.
Stretch*	Replace inner sleeve and housing.
Groove Width	Replace inner sleeve.
Material	Replace O-ring.

*See Figure 10 for Definition of Squeeze and Stretch.

temperature could also be achieved without any disassembly or re-assembly of parts, but a significant delay was involved since a stable, uniform condition had to be established before testing could be restarted at the new temperature. Further complexity was encountered at the highest temperature condition since the adhesive used to attach the accelerometers would soften and increase the likelihood of shaking loose one or more accelerometers. This problem did, in fact, limit the temperature at which data could be successfully taken to 216°C (420°F). All other changes in test conditions required some degree of disassembly and re-assembly. Of these a change to an O-ring of different material with the same cross-sectional diameter, or a change in squeeze, were most readily accomplished since these did not require a change of the sleeve or inner member (see Figure 10 for a definition of squeeze and stretch). To change the test parameters of O-ring cross-sectional diameter, groove width, or stretch required the most extensive disassembly since the inner sleeve had to be replaced.

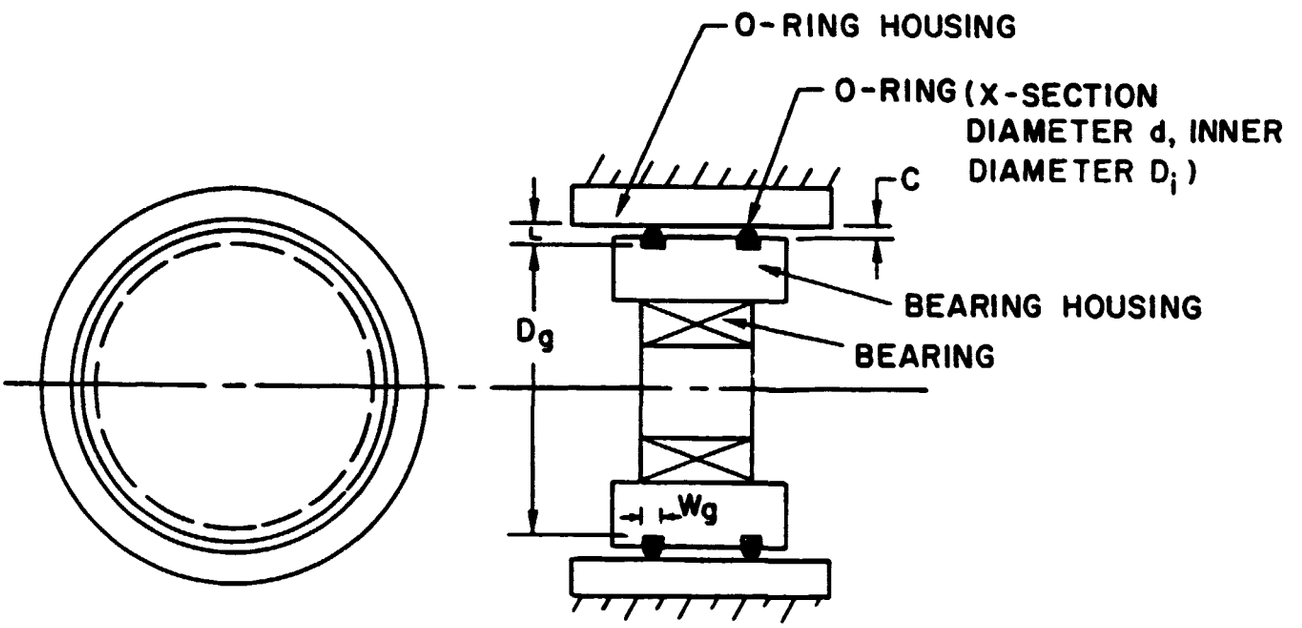

Fig. 10 Definition of Stretch and Squeeze

3.0 TEST RESULTS

The test plan undertaken was designed to provide maximum information for a minimum of test condition changes. With the large number of test parameters (7 + frequency), it was apparent that, unless a positive effort was made to hold the number of change of a minimum, a near endless test program could be required. To meet these constraints, a "parameter perturbation" approach was undertaken. Under this approach, a reference combination of all test parameters was defined and data for this reference combination was generated as a function of frequency. The reference condition is defined in Table 4. One single parameter was then varied about its reference value and data generated as a function of frequency for each variation. This parameter was then set back to its reference value and a second parameter varied about its reference value. This process was repeated for each of the seven parameters, in turn, and, by this test plan, the original reference condition became a reference for each parameter variation. The variation was repeated for each parameter, in turn, according to the schedule of Table 5, which resulted in a total of nineteen tests. An additional reference case or nominal test was performed with a different pair of rings, firstly to provide a check on repeatability from ring to ring and secondly because certain of the parameter perturbation tests (for temperature and amplitude) were performed with different O-rings, and it was deemed desirable to minimize the contributions of sample-to-sample variations in any observed trends.

The advantage of this parameter perturbation test method is that it returns a large amount of information from a small number of tests. The disadvantage is that it does not reveal the interactions which result from varying more than one parameter at a time. Thus, the results of this series of tests should be regarded as a baseline set of data from which major trends and influential parameters can be identified. The less significant parameters can be identified and eliminated from further tests in which interaction effects between parameters are investigated.

The test frequency range generally lay between 70 and 1,000 Hz. Some data was obtained below 70 Hz, and it was possible to obtain resonant condition as low as 20 Hz with a high mass. It was found, however, that significant rocking of the mass occurred and, because of the low accelerations involved in a 0.3 mil amplitude at these frequencies, the data was not considered of sufficient reliability to be included in this report.

TABLE 4

REFERENCE OR NOMINAL TEST CONDITION

Material. . . .	Viton-70	Stretch	5 percent
Temperature . .	25°C	X-Section Diameter. .	1/8" Nominal (0.353 cm**)
Amplitude . . .	7.62×10^{-6} m	Groove Width*	135 percent
Squeeze	15 percent	O-Ring OD	2-1/2" Nominal (6.35 cm)

*Based on actual X-Section diameter

**Measured Average

TABLE 5

PERTURBATION PARAMETER VALUES

Material	Buna-N		Viton-90		
Temperature	38°C	66°C	149°C	216°C	
Amplitude	2.54×10^{-5} m		1.27×10^{-4} m		(1 mil, 5 mils)
Squeeze	5%	10%	20%	30%	
Stretch	0%	10%			
X-Section Diameter	1/16" nominal (1.778×10^{-3} m) 3/16" nominal (5.334×10^{-3} m)				
Groove Width	115%	150% of actual X-Section diameter			

As a result of this test program, twenty conditions were tested in all, two nominal and 18 parameter perturbations. Data for each condition was acquired by the automated data acquisition system, stored on disk, and after the test was complete, presented as a neat, ordered, tabulation versus frequency. Plots of these data have been prepared for each test condition and are presented in Figures 11 through 30 (one per test condition). In each of these 20 figures there are two frames: one for loss coefficient (k"/k') and one for stiffness (k' in N/m) where k', k" are stiffness and damping. Each frame has log/log axes with frequency in Hertz as the abscissa. Actual test data points are shown in each case and through the full set of data points is drawn a power law line which gives the minimum RMS deviation between test data and the fitted line. All plots of stiffness are for a pair of O-rings, as tested, since this is the most likely configuration to be encountered in practice.

With reference to these plots of actual test data, discussion will be limited to data quality and general characteristics. Comparative trends will be discussed with reference to the "trend summary plots" which follow.

The quality of the data is considered to be good, with acceptable scatter. Use of the power law fit is justified, in that no consistent trend other than a linear variation on the log/log scale is discernable in the data, over the frequency range tested. Figures 11 and 12 indicate reasonable repeatability of stiffness between nominally similar O-rings (1.8 percent discrepancy at 100 Hz and 5.2 percent discrepancy at 1,000 Hz between law lines). Similar repeatability is observed in loss coefficient (5 percent discrepancy at 100 Hz and 1.7 percent discrepancy at 1,000 Hz between power law lines).

Significant characteristics of most of the data are a strong increase in stiffness with frequency (typically by a factor of 2.5) and a high value of loss coefficient (in the range of 0.7 to 1.1). Of further interest is the fact that the 1,000 Hz stiffness is over 9 times the static stiffness of a pair of O-rings (static stiffness measurement will be discussed below). These characteristics are indicative of an elastomer in its transition region (5) and are consistent with others measured for Viton (6).

MATERIAL: VITON-70
TEMPERATURE: 25° C
AMPLITUDE: 7.62×10^{-6} m
SQUEEZE: 15%

X-SECTION DIA.: 1/8 IN. (.353 cm.)
STRETCH: 5%
GROOVE WIDTH: 135%

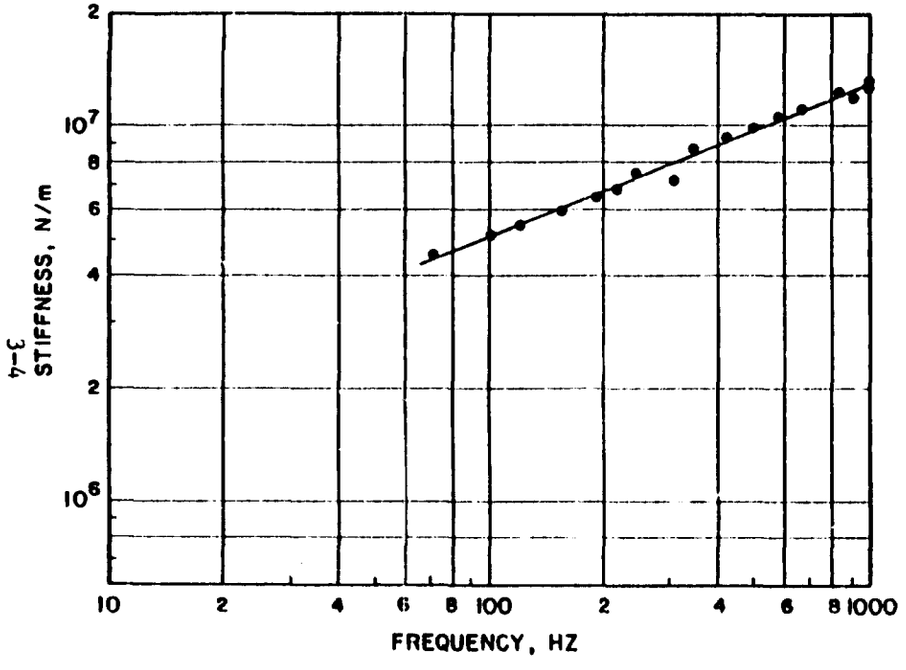

(A)

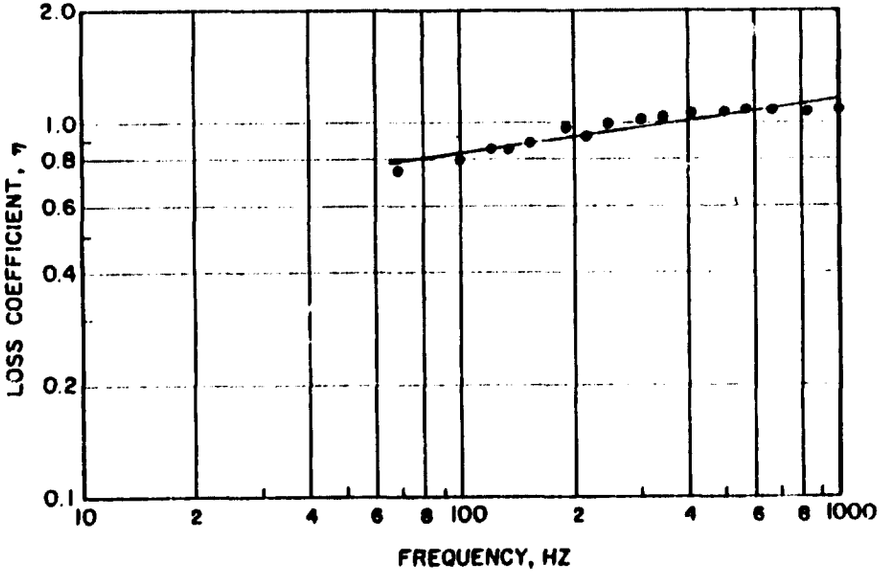

(B)

Fig. 11 Test Results: Nominal Case

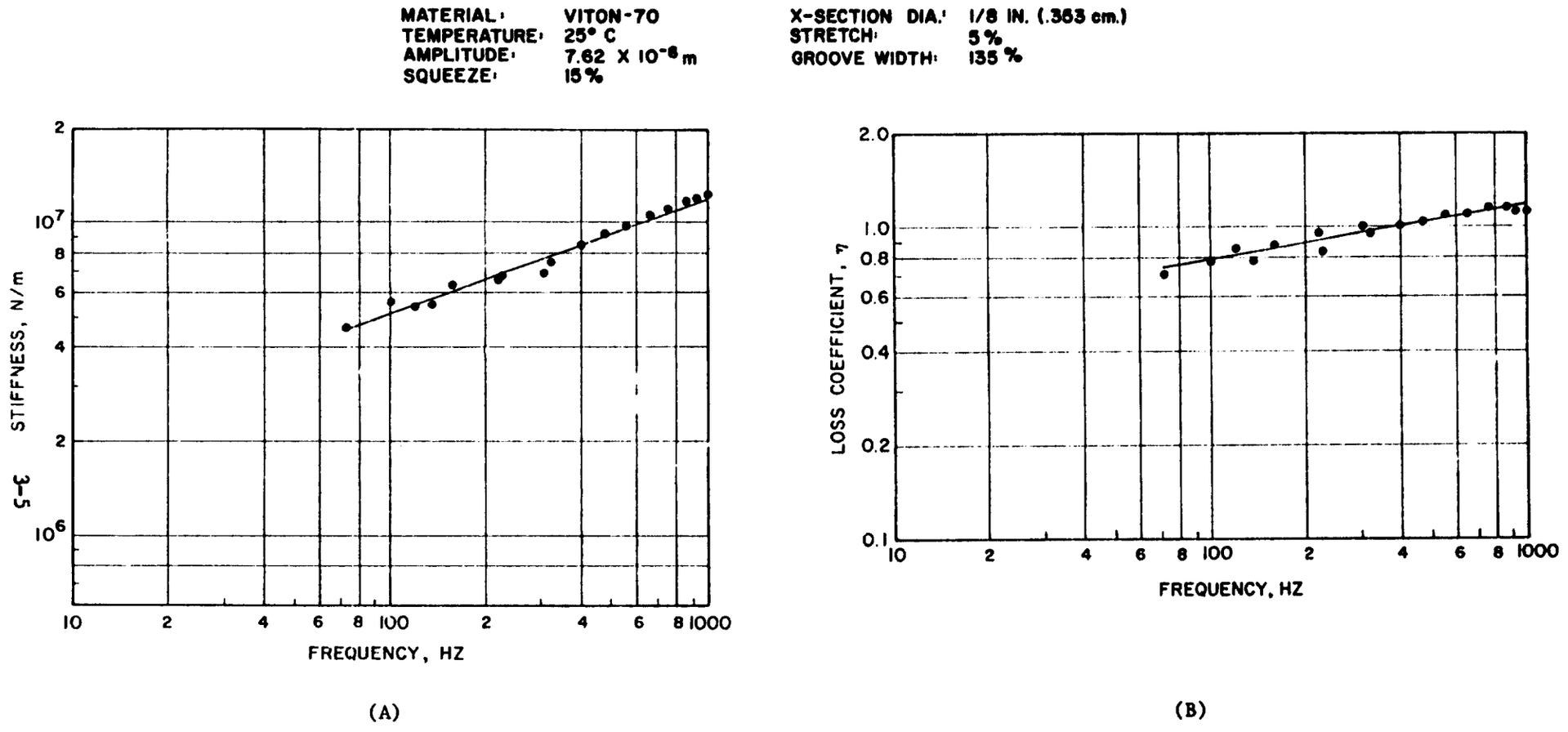

Fig. 12 Test Results: Nominal Case

MATERIAL: BUNA-N
TEMPERATURE: 25° C
AMPLITUDE: 7.62 X 10^{-6} m
SQUEEZE: 15%

X-SECTION DIA.: 1/8 IN. (.353 cm)
STRETCH: 5%
GROOVE WIDTH: 135%

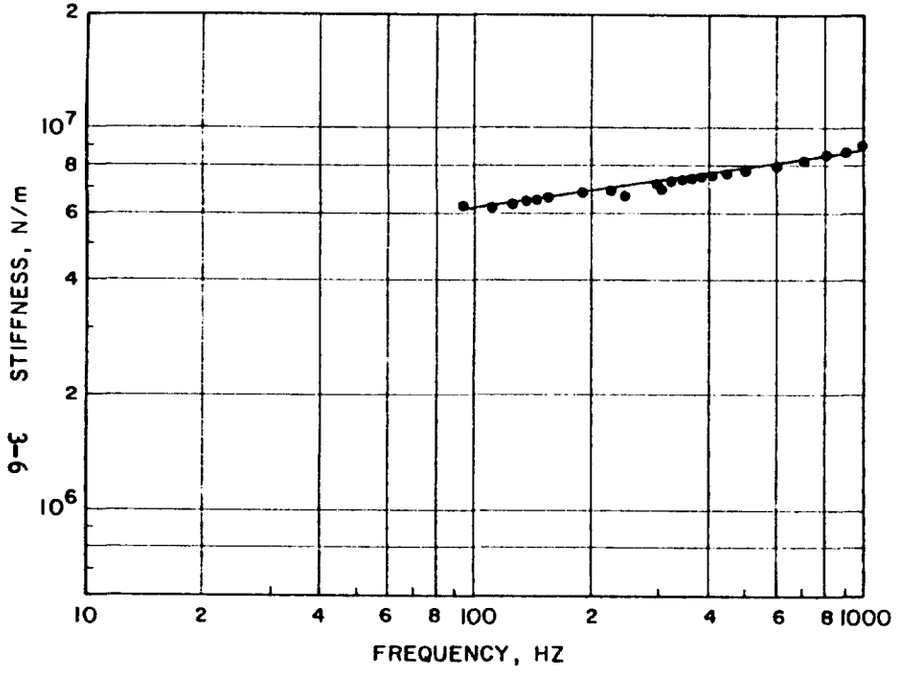

(A)

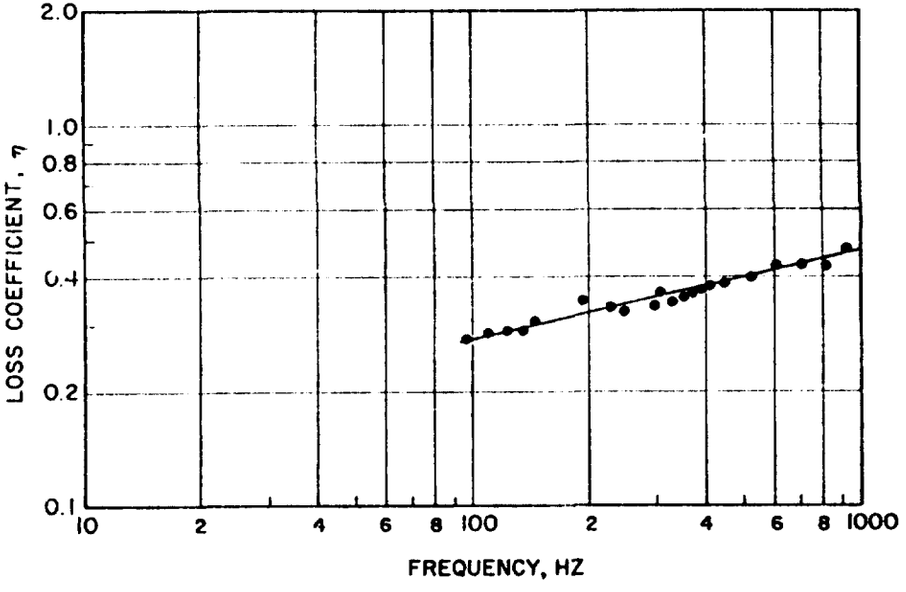

(B)

Fig. 13 Test Results: Buna-N

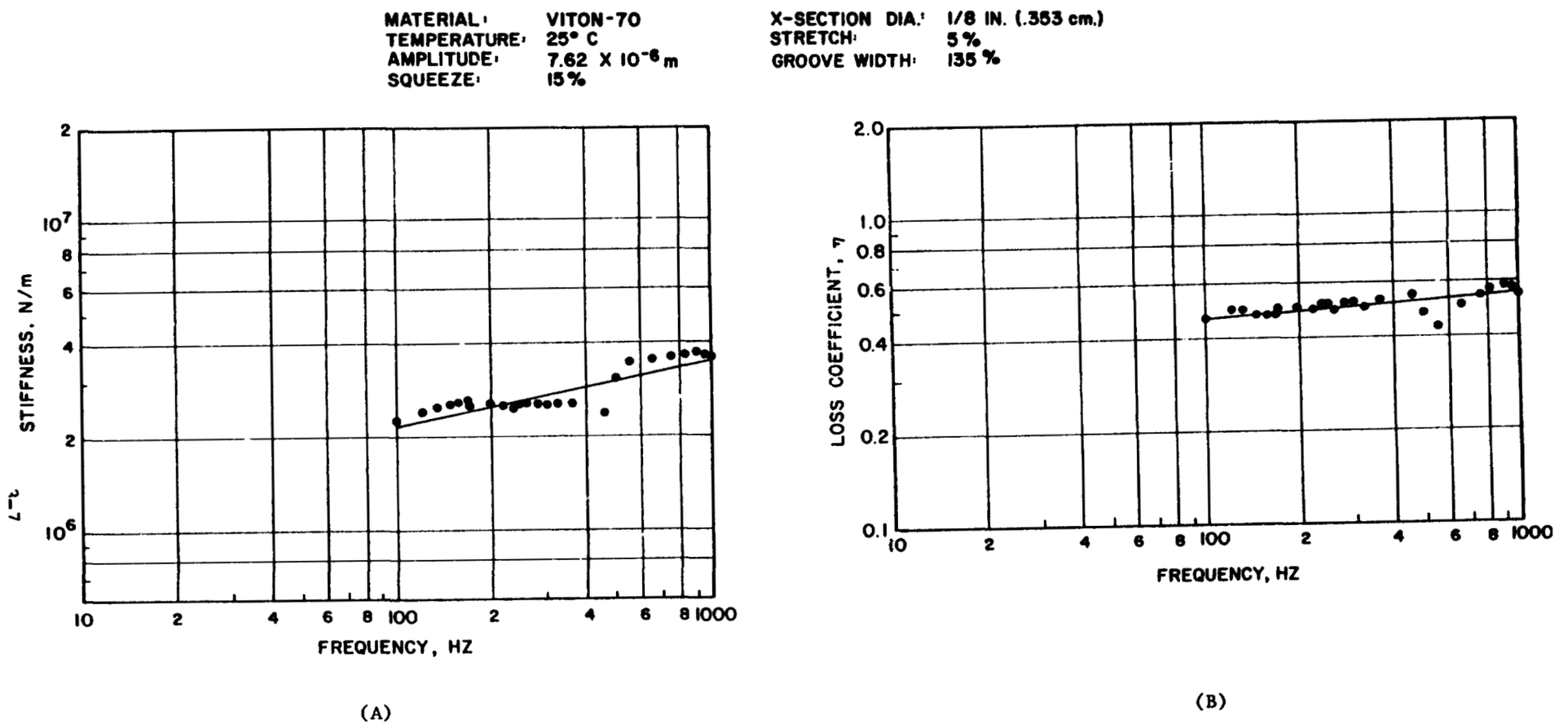

(A) (B)

Fig. 14 Test Results: Viton-90

MATERIAL: VITON-70
TEMPERATURE: 38° C
AMPLITUDE: 7.62 X 10^{-6} m
SQUEEZE: 15%

X-SECTION DIA.: 1/8 IN. (.353 cm)
STRETCH: 5%
GROOVE WIDTH: 135%

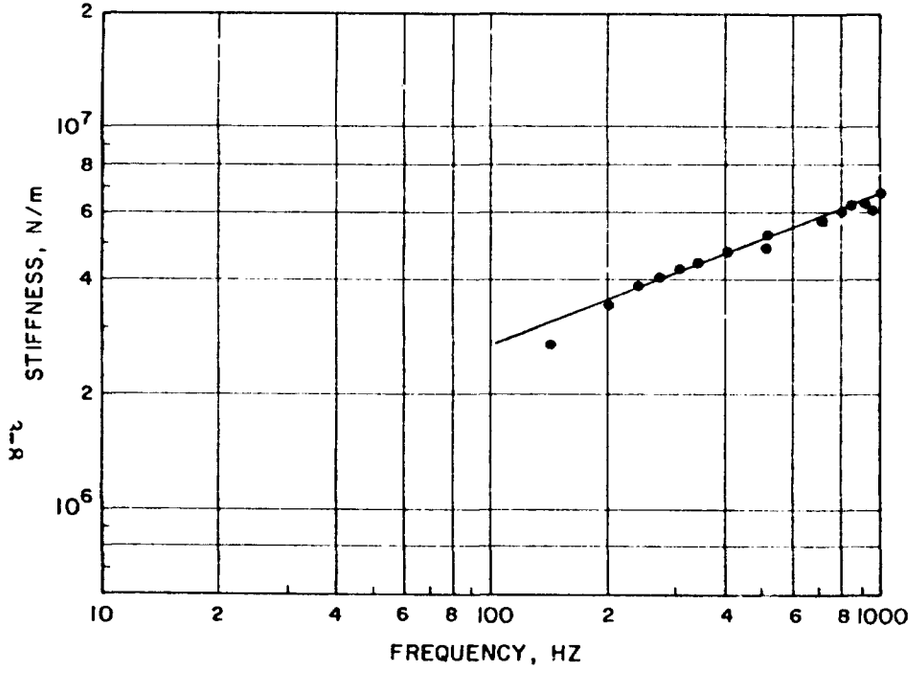

(A)

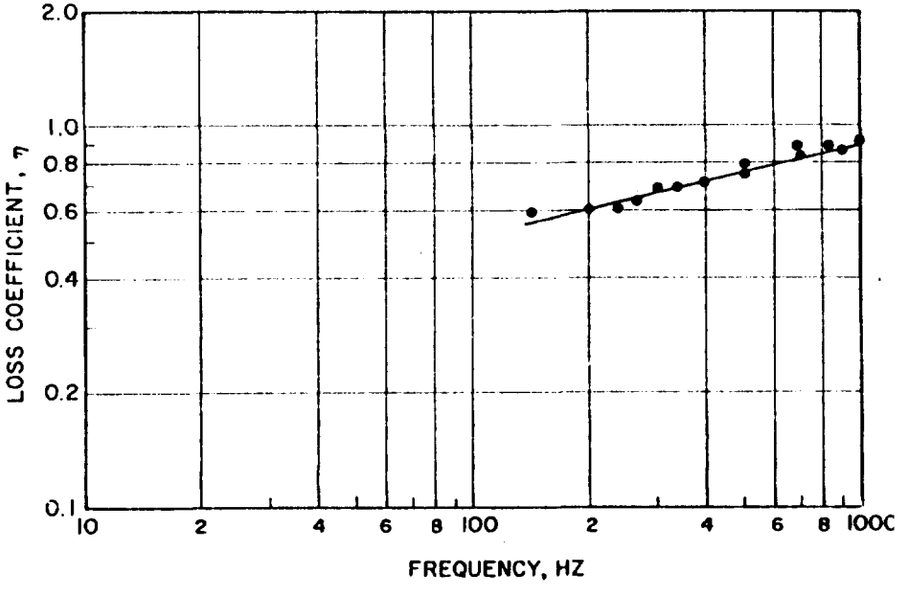

(B)

Fig. 15 Test Results: Temperature 38°C

MATERIAL:	VITON-70	X-SECTION DIA.:	1/8 IN. (.353 cm)
TEMPERATURE:	66° C	STRETCH:	5 %
AMPLITUDE:	7.62 X 10^{-6} m	GROOVE WIDTH:	135 %
SQUEEZE:	15 %		

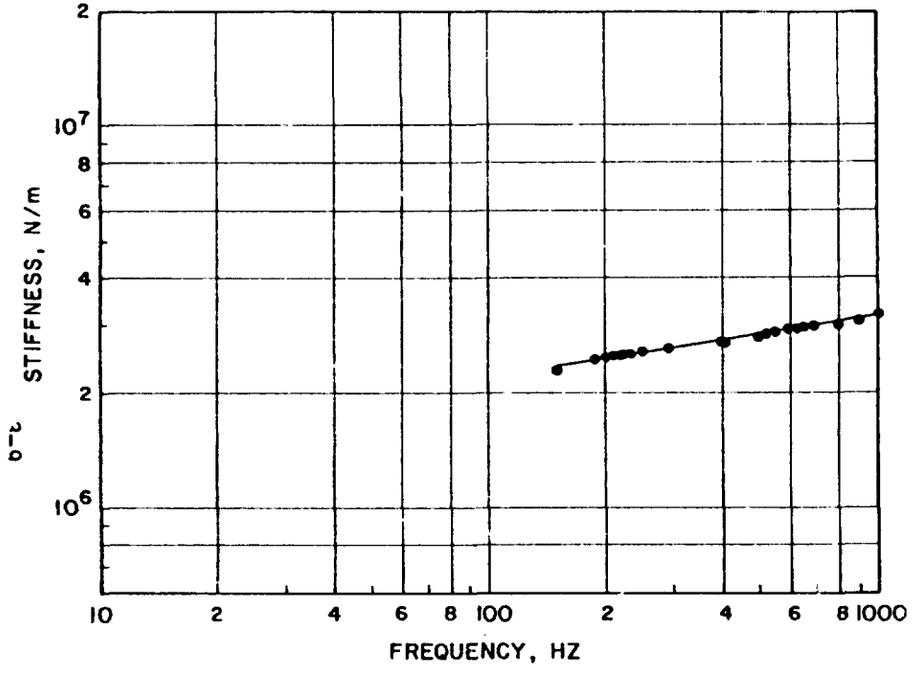

(A)

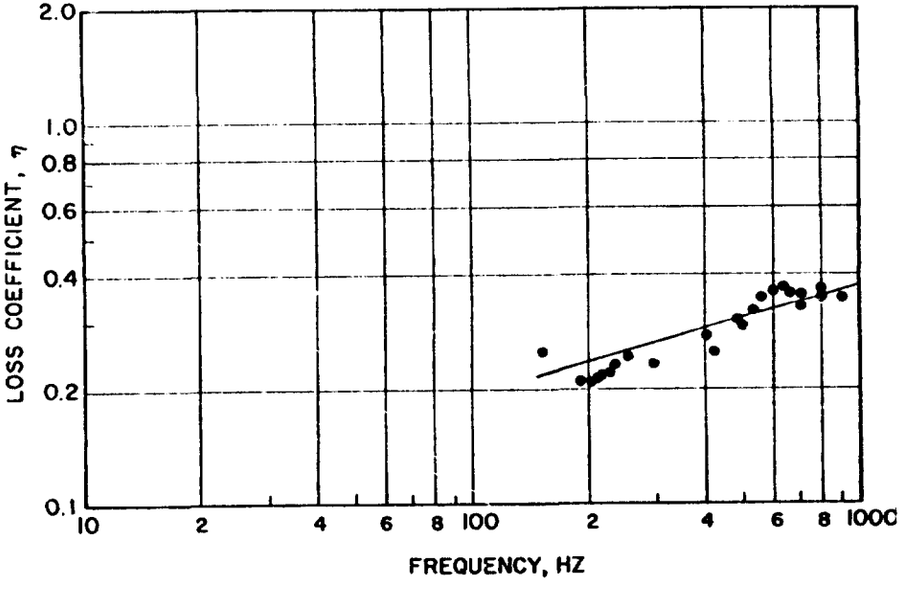

(B)

Fig. 16 Test Results: Temperature 66°C

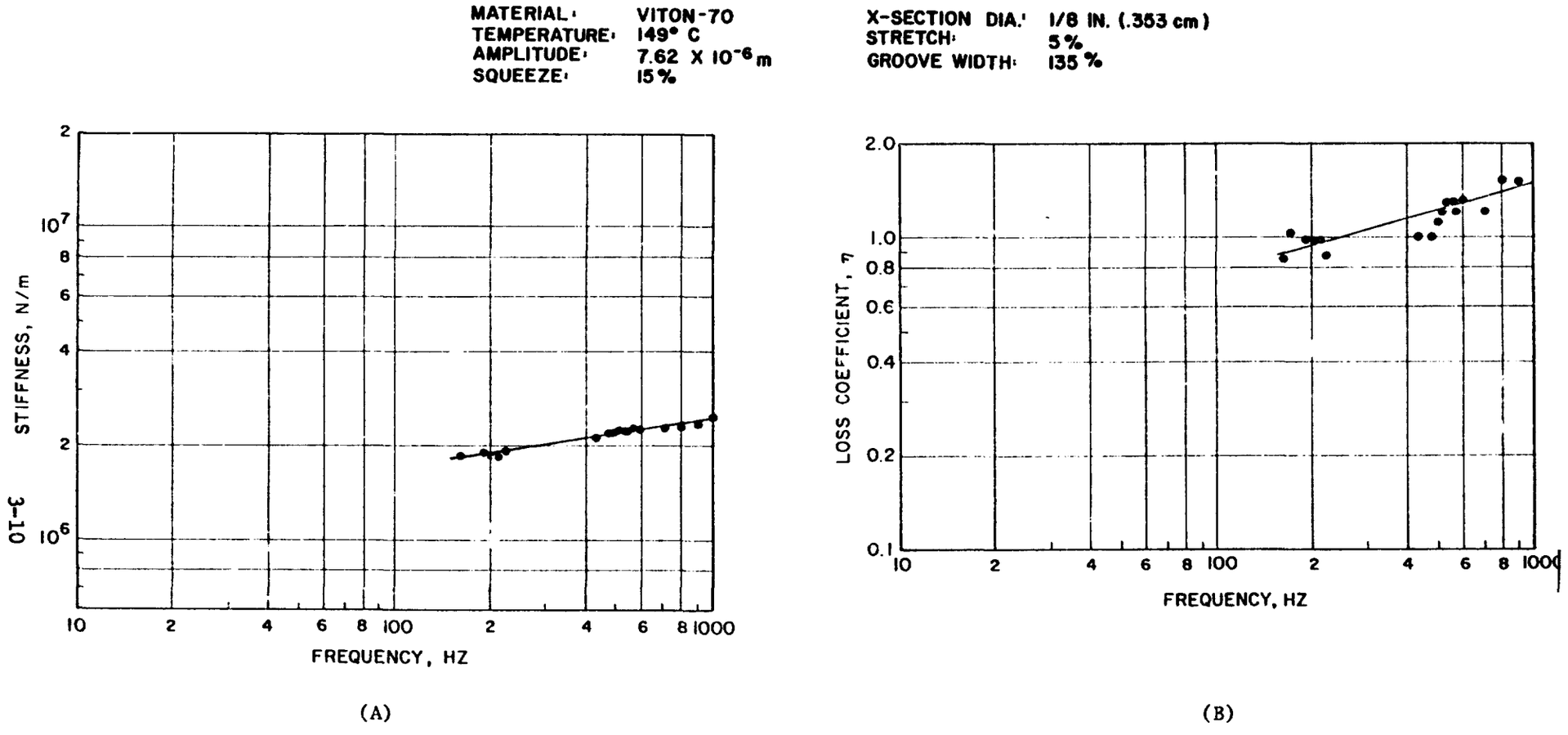

Fig. 17 Test Results: Temperature 149°C

MATERIAL: VITON-70
TEMPERATURE: 216° C
AMPLITUDE: 7.62 X 10^{-6} m
SQUEEZE: 15%

X-SECTION DIA.: 1/8 IN. (.353 cm.)
STRETCH: 5%
GROOVE WIDTH: 135%

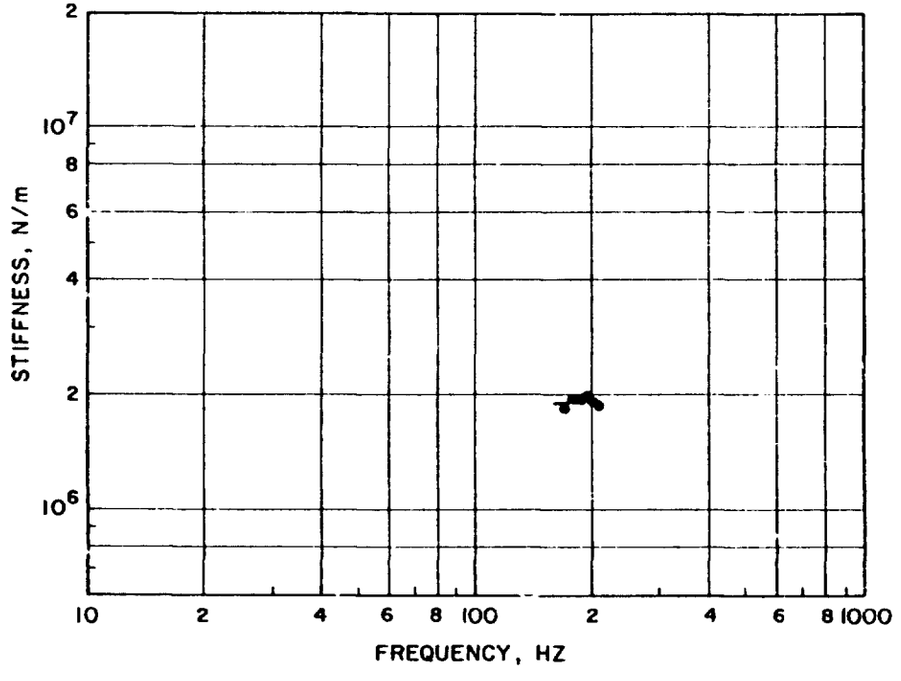

(A)

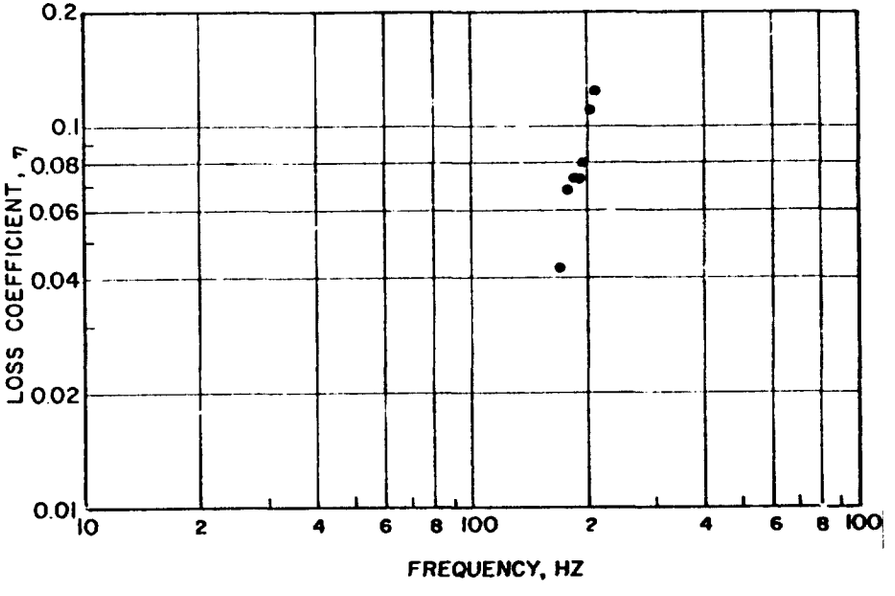

(B)

Fig. 18 Test Results: Temperature 216°C

MATERIAL: VITON-70
TEMPERATURE: 25° C
AMPLITUDE: 25.4 X 10^{-6}m
SQUEEZE: 15%

X-SECTION DIA.: 1/8 IN. (.353 cm)
STRETCH: 5%
GROOVE WIDTH: 135%

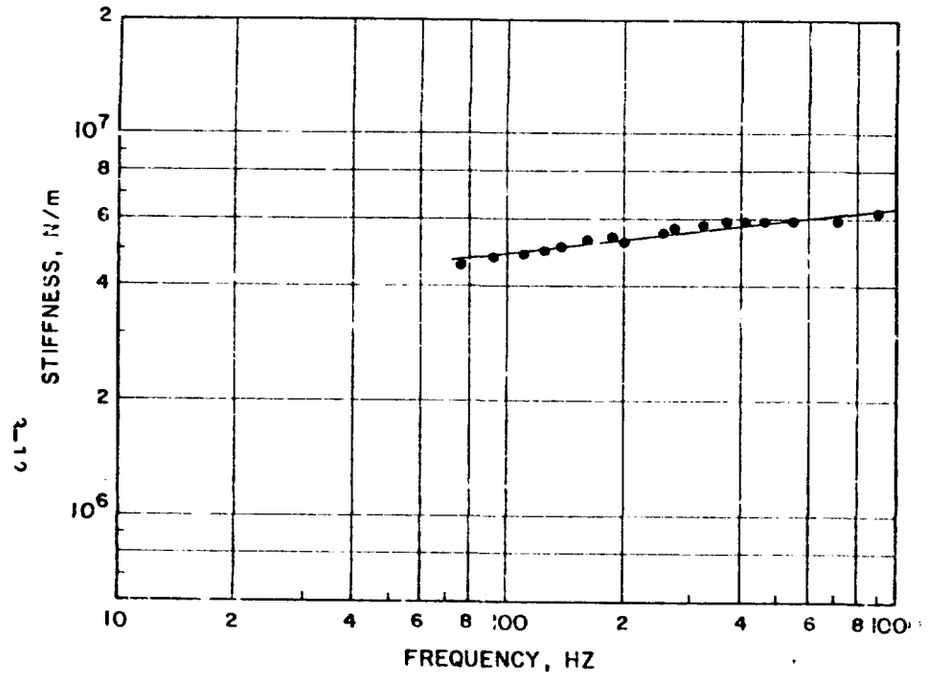

(A)

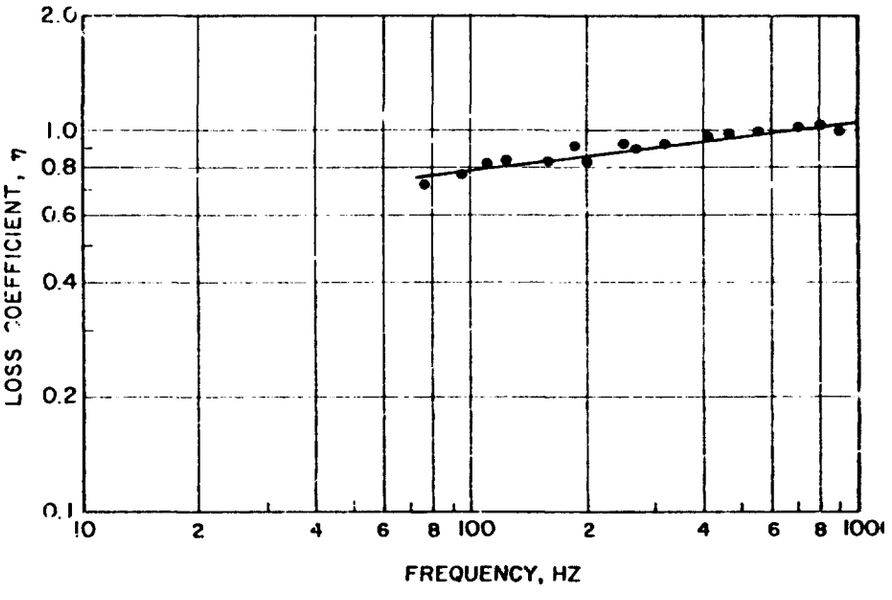

(B)

Fig. 19 Test Results: Amplitude, 1 mil

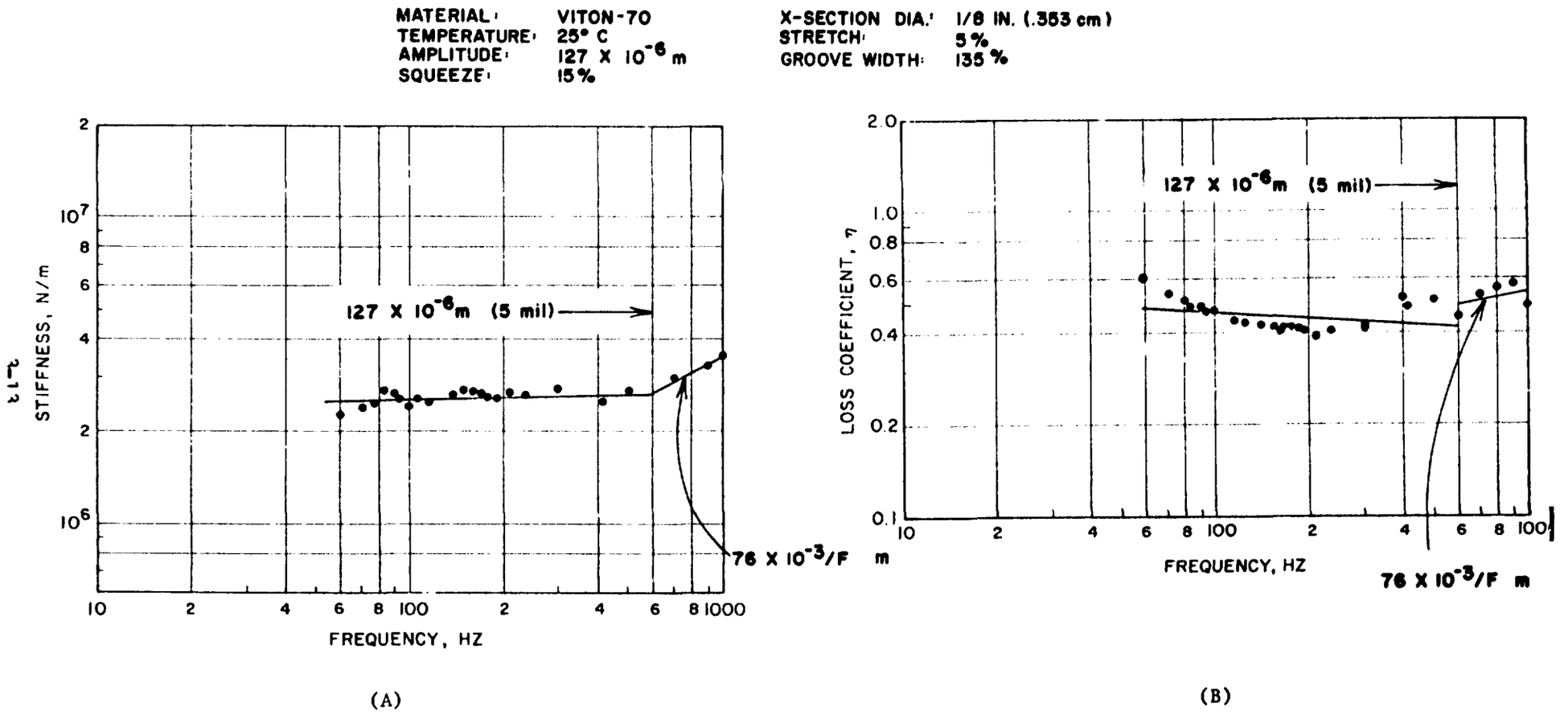

Fig. 20 Test Results: Amplitude, 5 mil

MATERIAL: VITON-70
TEMPERATURE: 25° C
AMPLITUDE: 7.62 X 10^{-6} m
SQUEEZE: 5%

X-SECTION DIA.: 1/8 IN. (.353 cm)
STRETCH: 5%
GROOVE WIDTH: 135 %

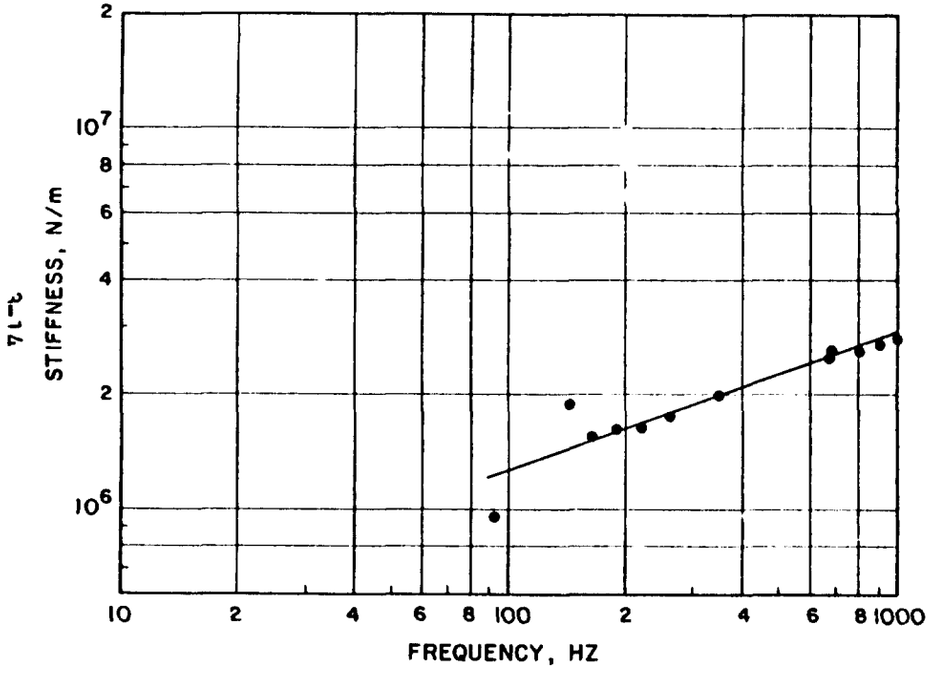

(A)

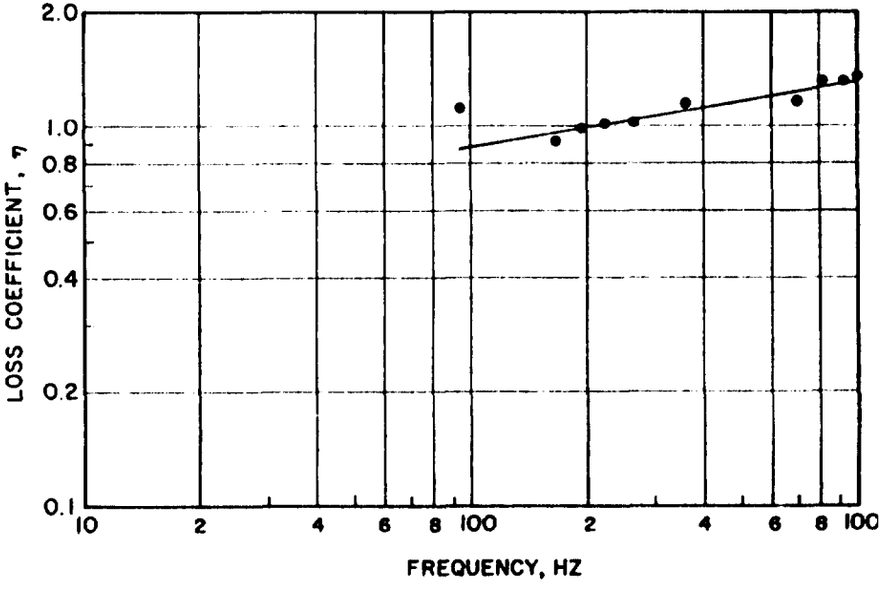

(B)

Fig. 21 Test Results: Squeeze, 5%

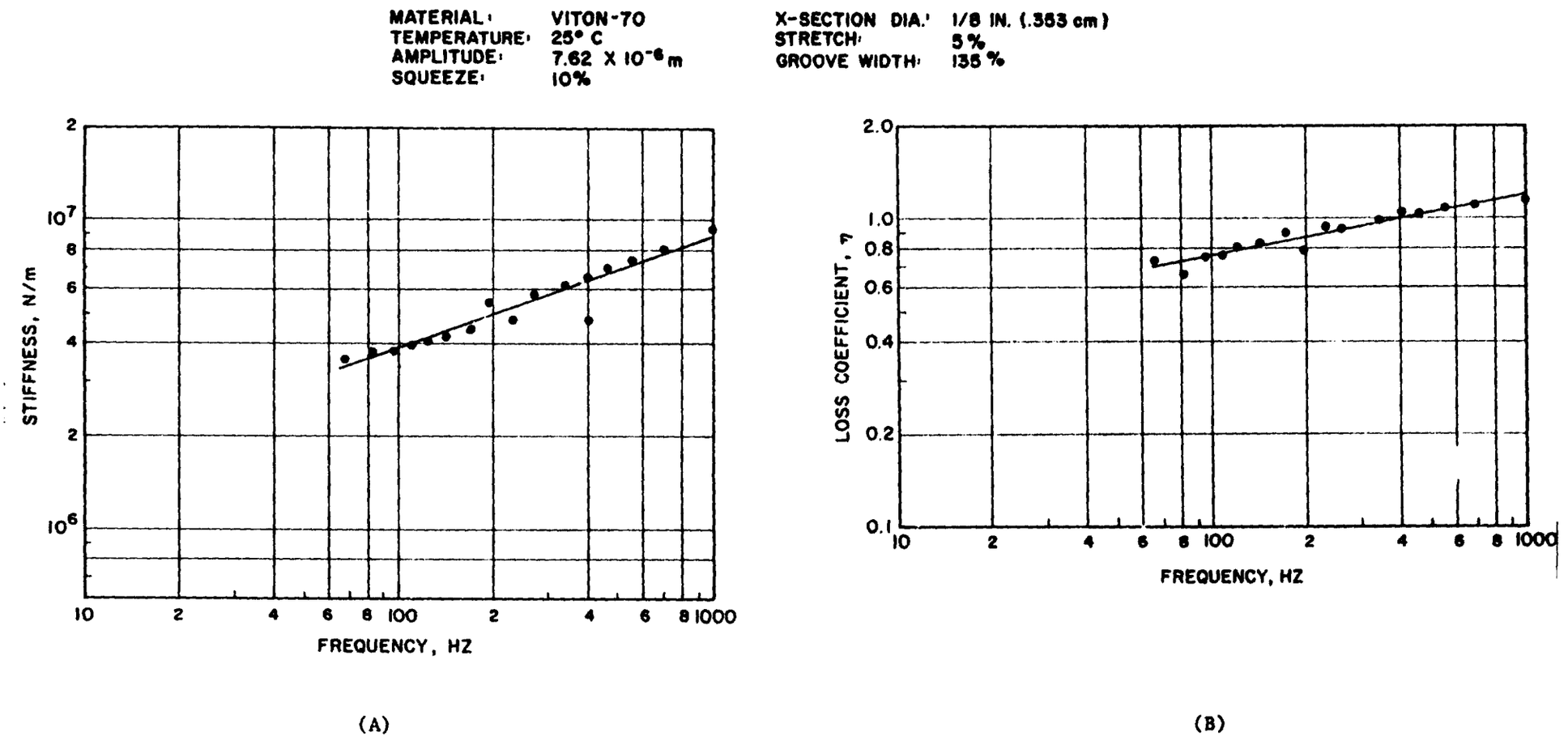

Fig. 22 Test Results: Squeeze, 10%

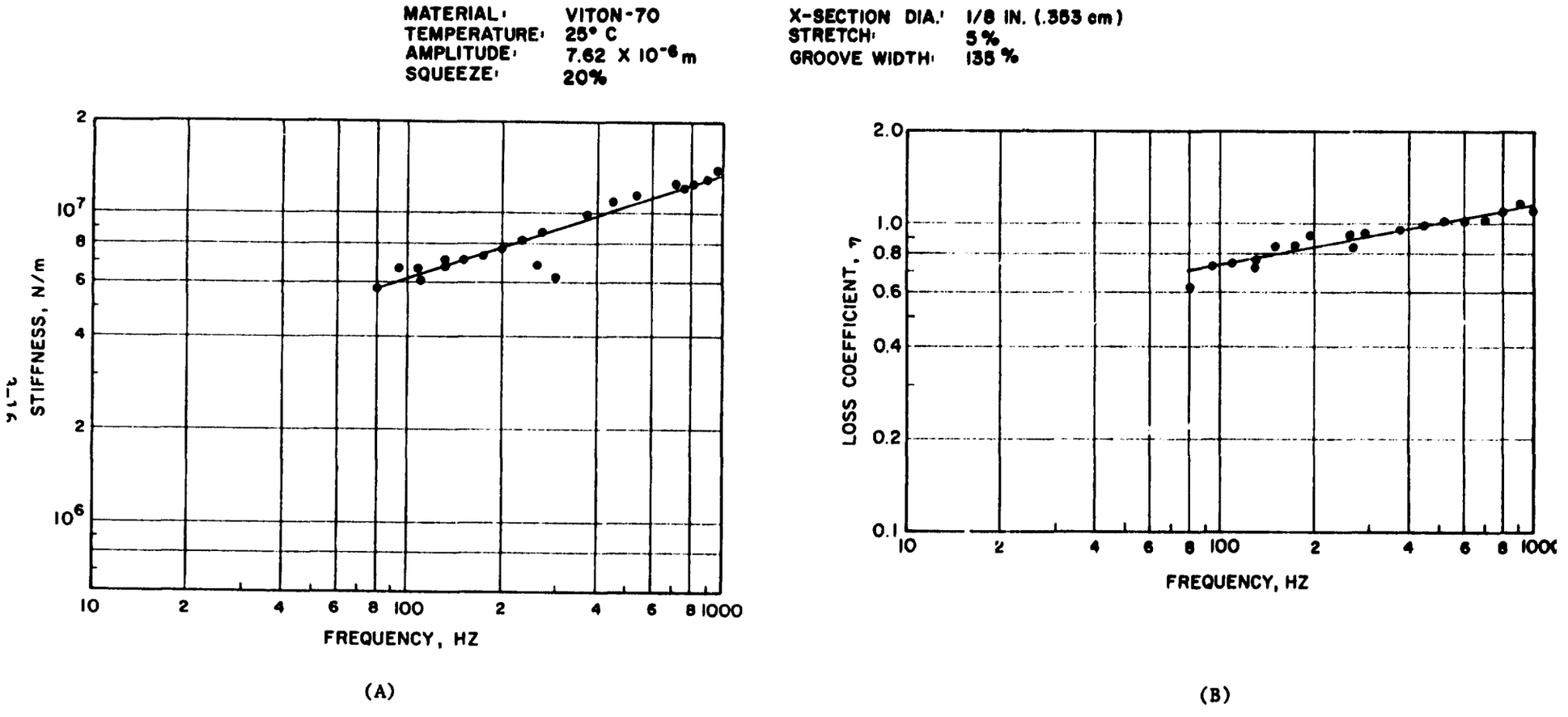

Fig. 23 Test Results: Squeeze, 20%

MATERIAL: VITON-70
TEMPERATURE: 25° C
AMPLITUDE: 7.62 X 10^{-6} m
SQUEEZE: 30%

X-SECTION DIA.: 1/8 IN. (.353 cm)
STRETCH: 5%
GROOVE WIDTH: 135 %

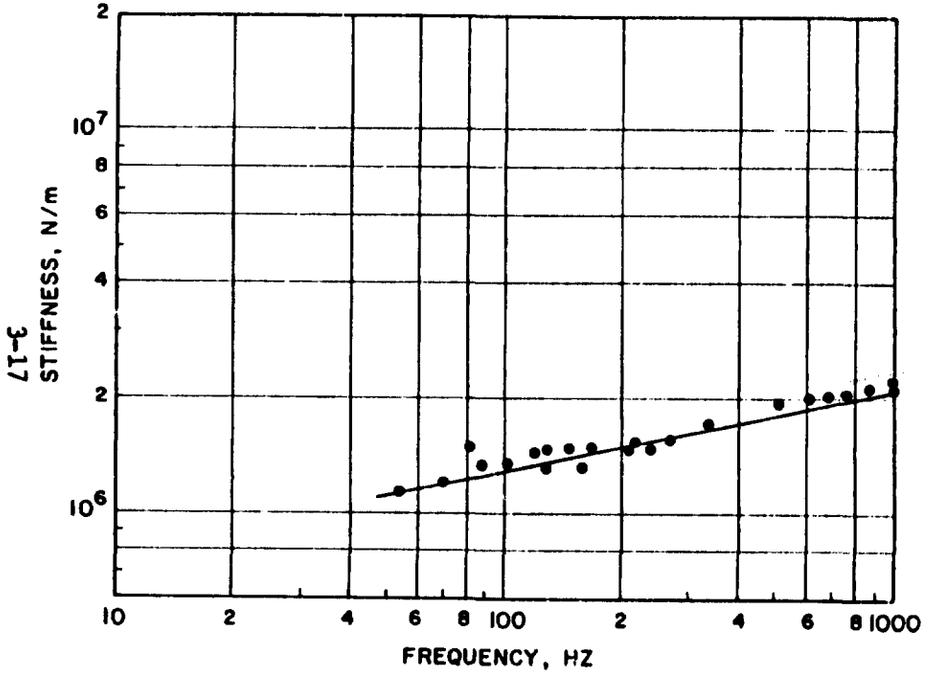

(A)

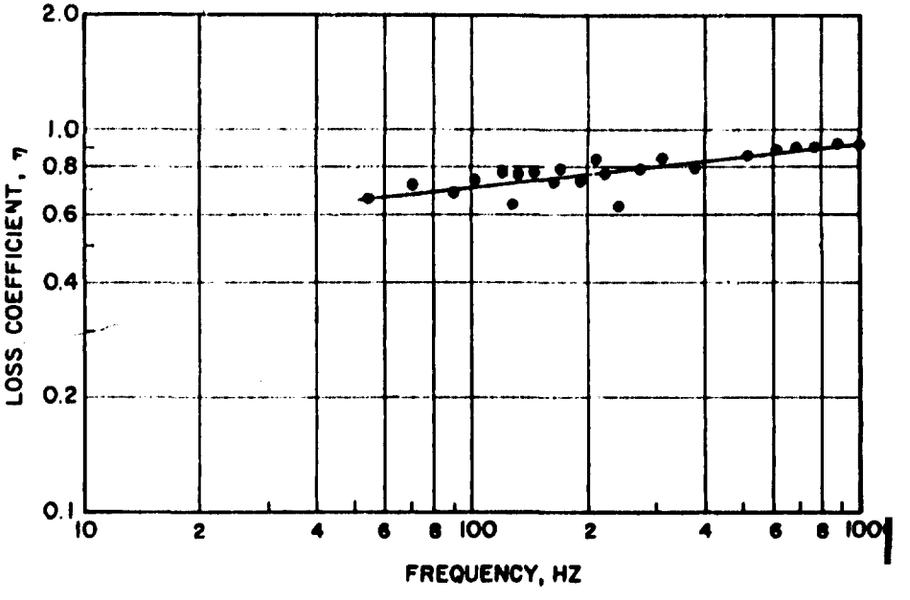

(B)

Fig. 24 Test Results: Squeeze, 30%

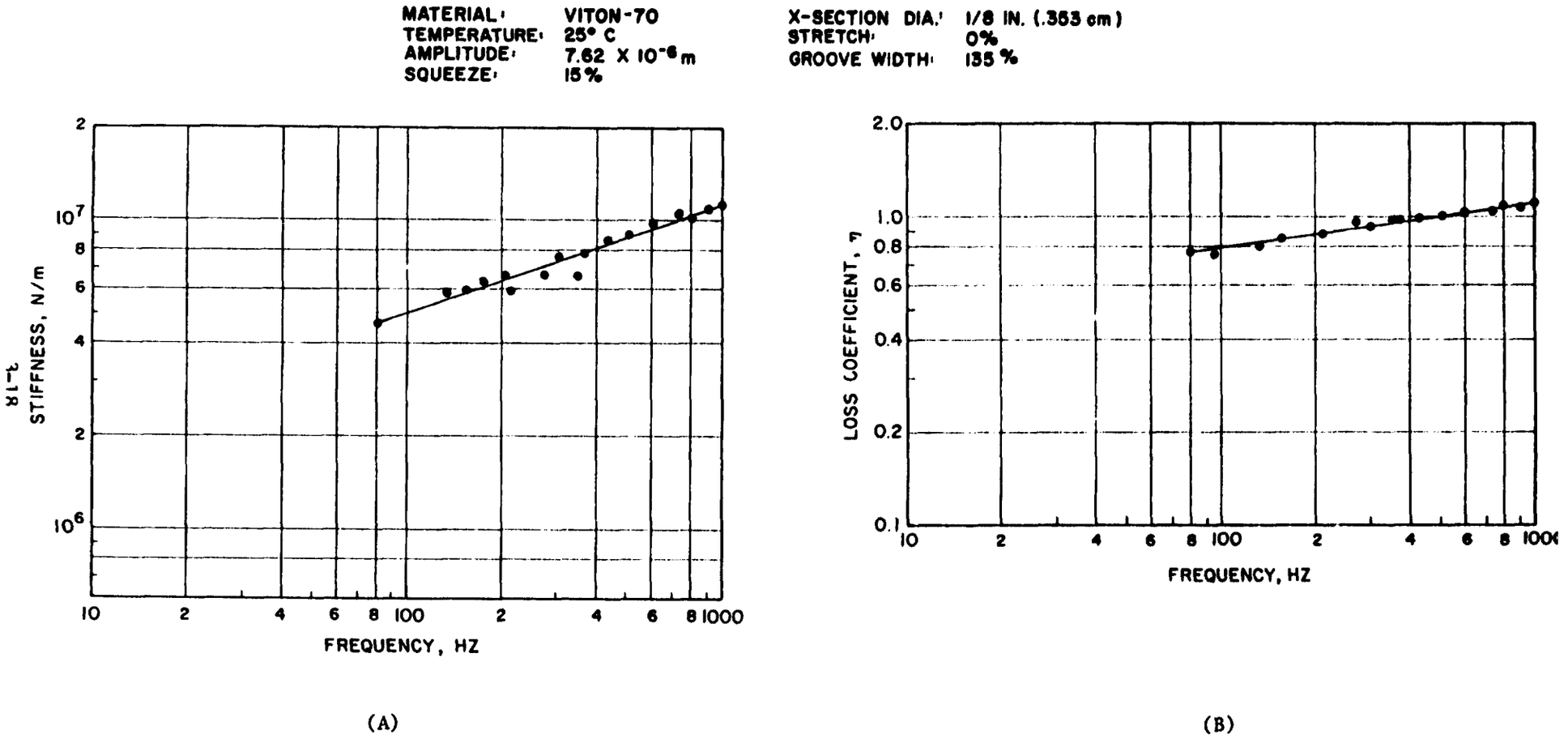

Fig. 25 Test Results: Stretch, 0%

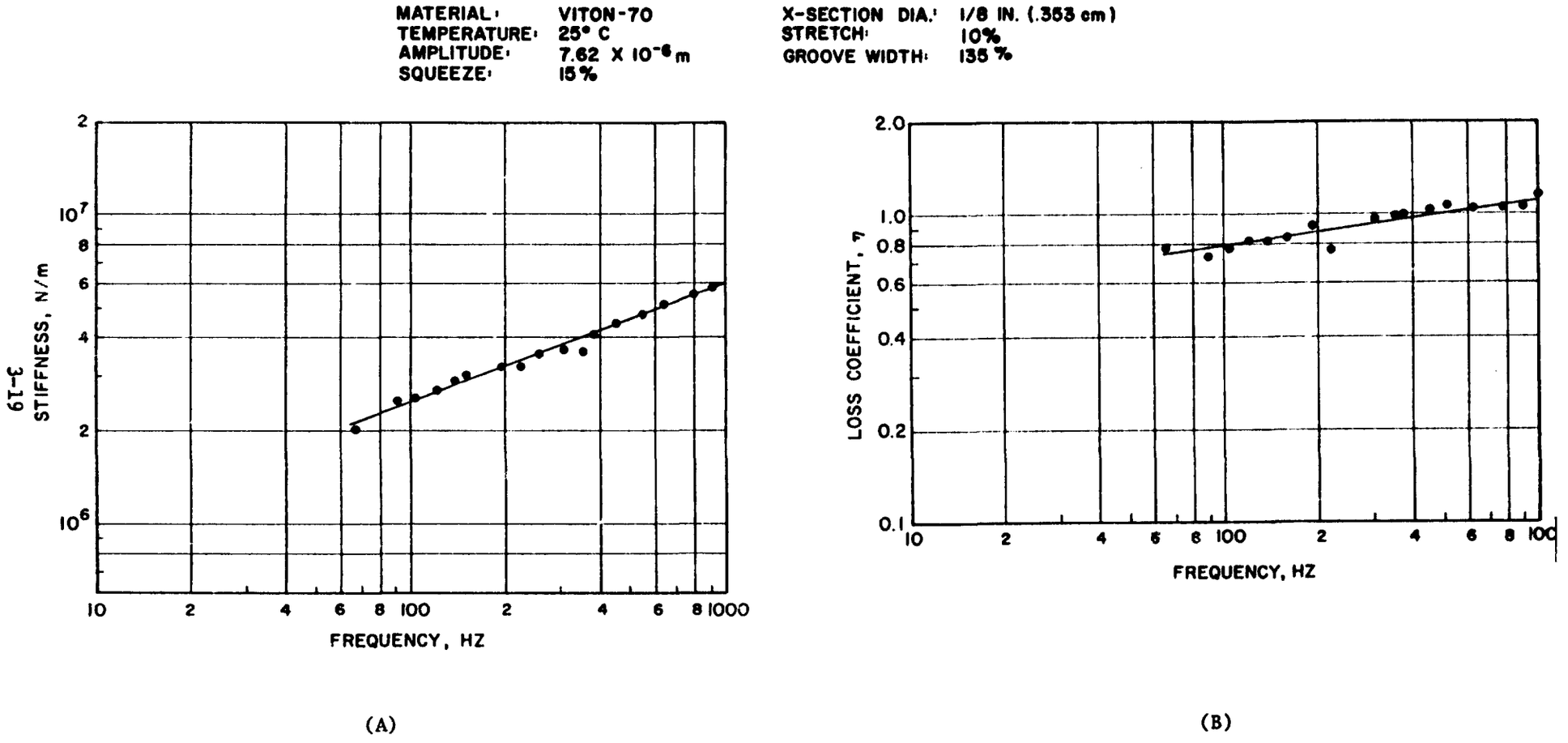

Fig. 26 Test Results: Stretch, 10%

MATERIAL: VITON-70
TEMPERATURE: 25° C
AMPLITUDE: 7.62 X 10^{-6} m
SQUEEZE: 15%

X-SECTION DIA.: 1/16 IN. (.178 cm)
STRETCH: 5%
GROOVE WIDTH: 135%

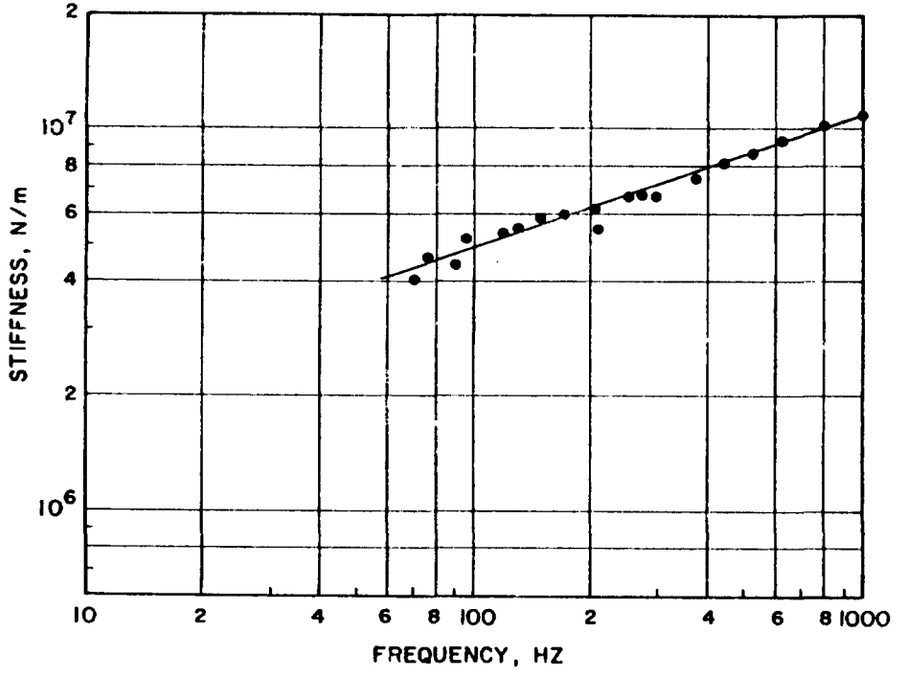

(A)

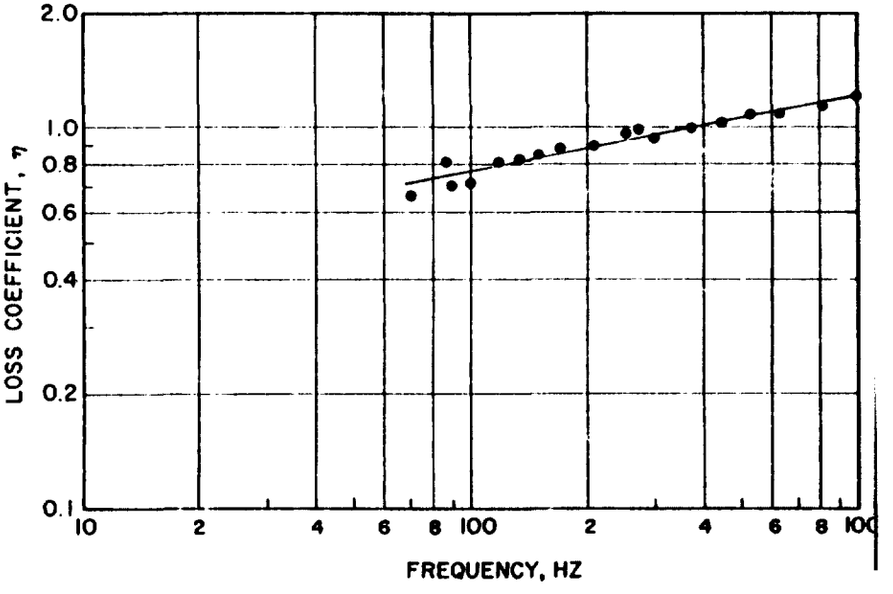

(B)

Fig. 27 Test Results: Nominal Cross-Section, 1/16 in.

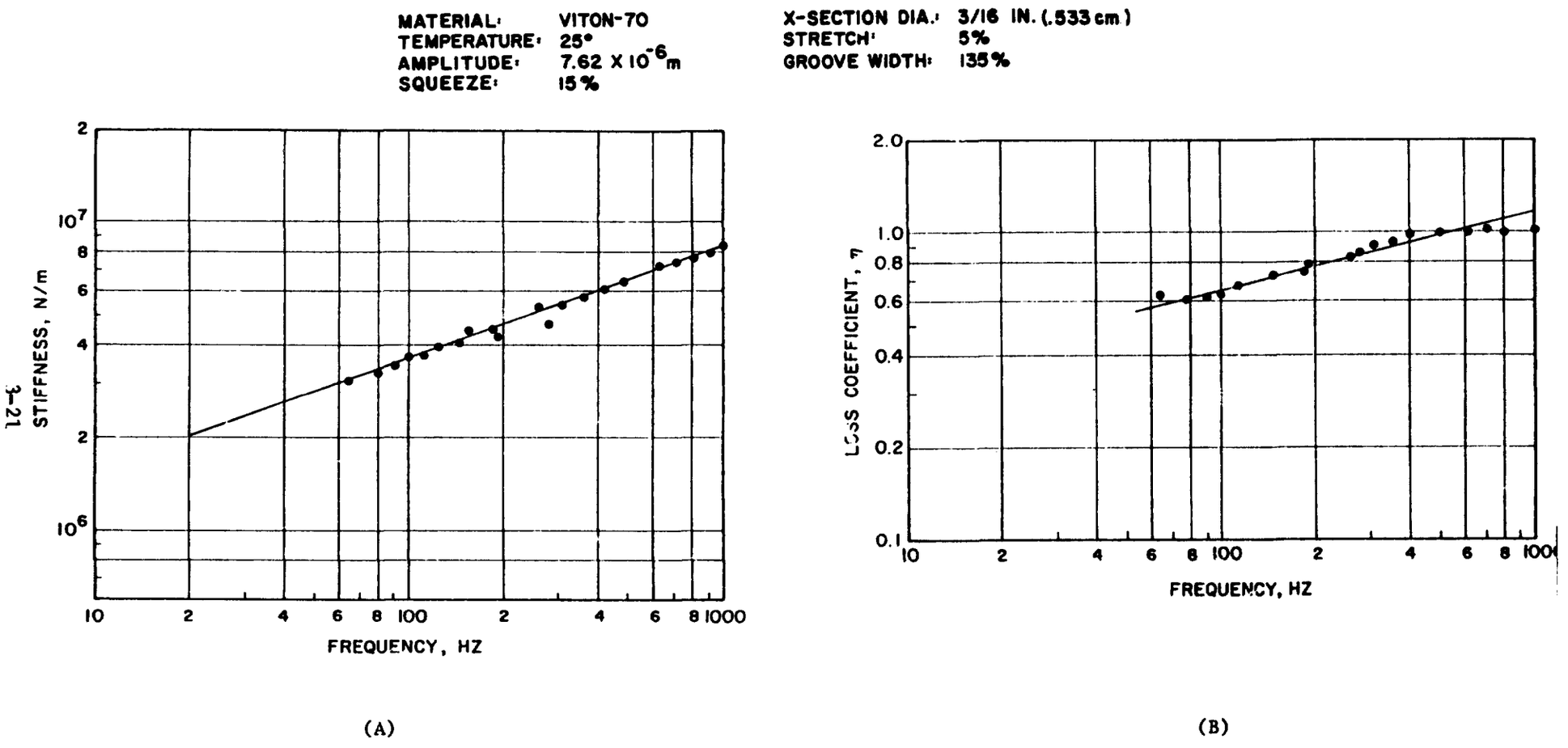

Fig. 28 Test Results: Nominal Cross-Section, 3/16 in.

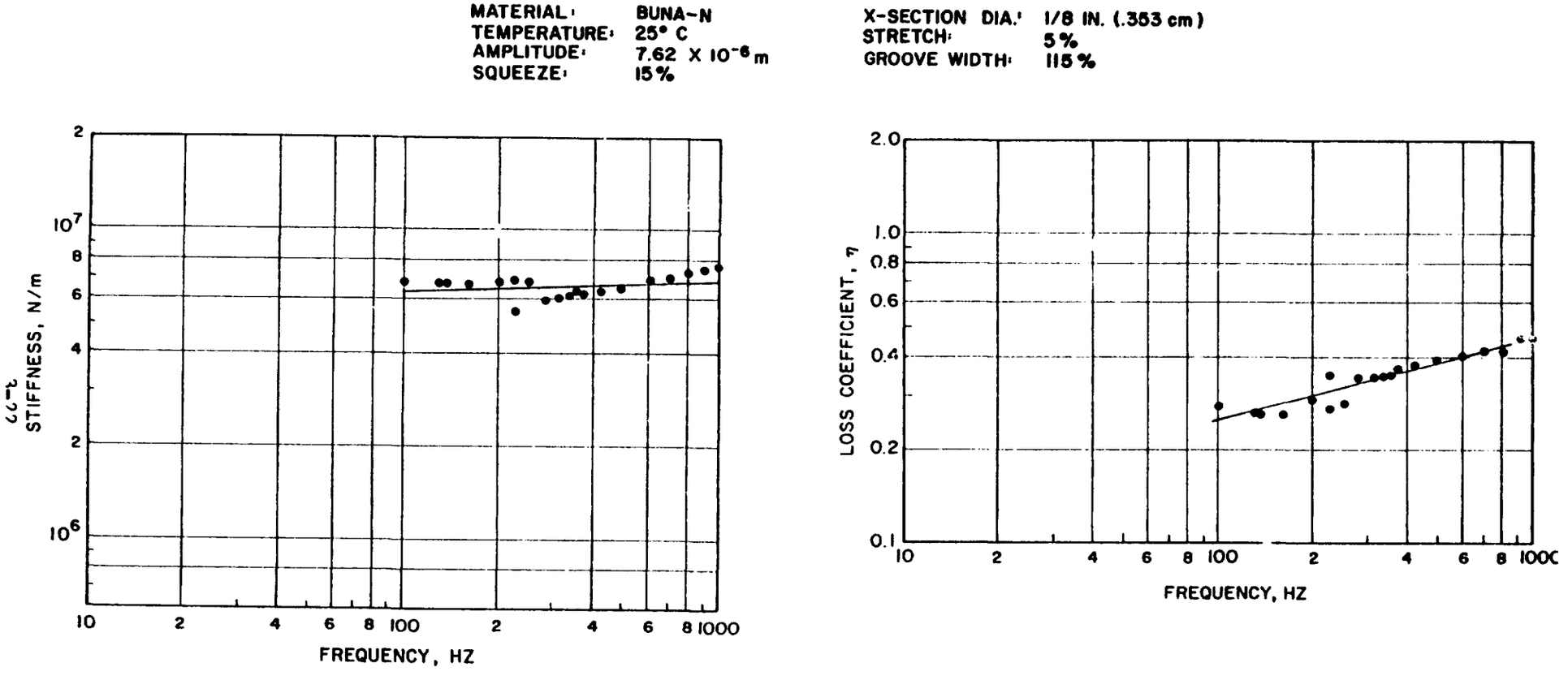

(A) (B)

Fig. 29 Test Results: Grove Width, 115%

MATERIAL: BUNA-N
TEMPERATURE: 25° C
AMPLITUDE: 7.62 X 10^{-6} m
SQUEEZE: 15%

X-SECTION DIA.: 1/8 IN. (.353 cm)
STRETCH: 5%
GROOVE WIDTH: 150%

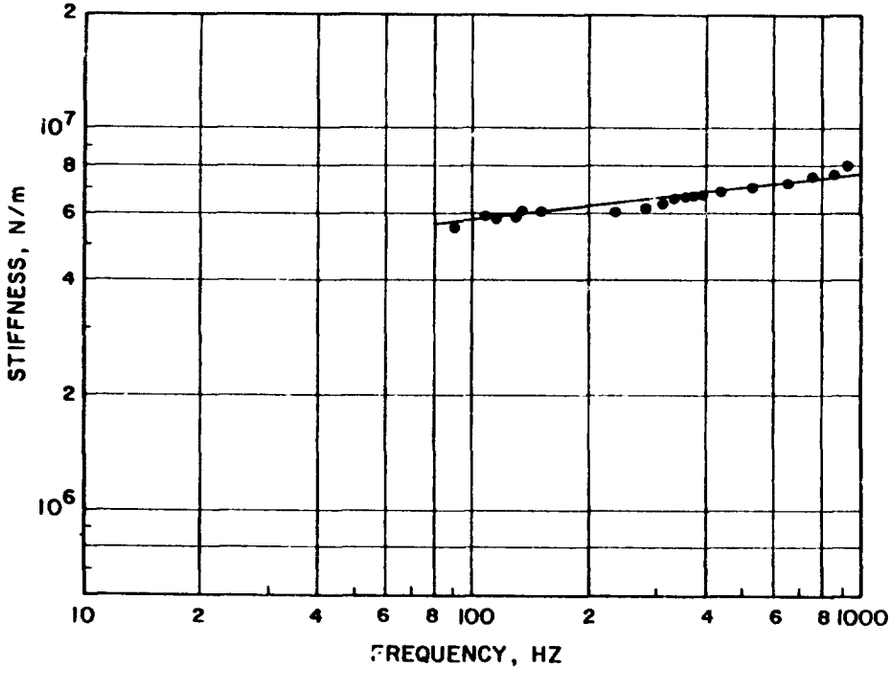

(A)

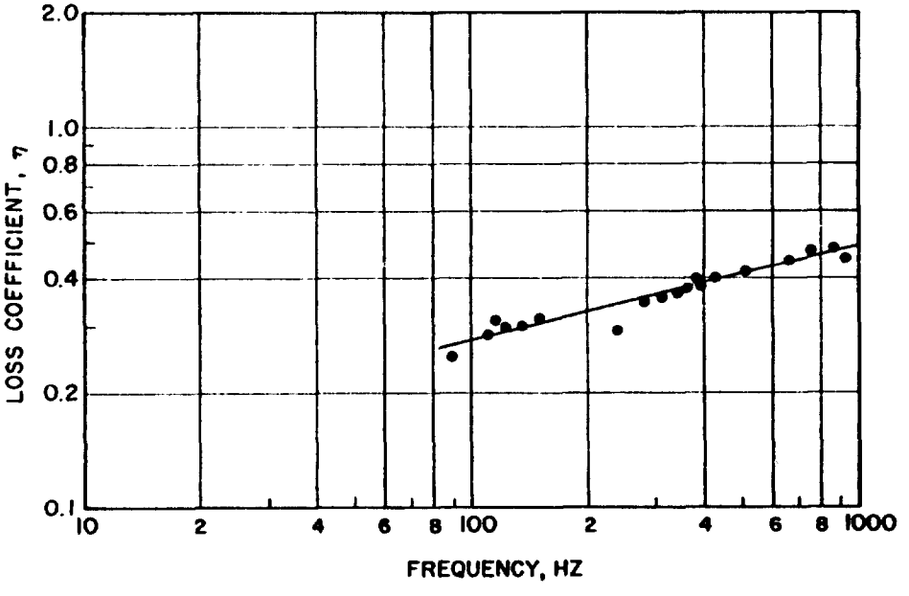

(B)

Fig. 30 Test Results: Groove Width, 150%

Summary of Fitted Analytical Expressions

For use in design and for comparative purposes, it is useful to have algebraic expressions available for stiffness and loss coefficient. For this reason, in Table 6 are presented the values of coefficients, for stiffness and loss coefficient, corresponding to each of the fitted power law lines shown in Figures 11 through 30. To apply these coefficients in finding stiffness, loss coefficient, or damping at a particular frequency, f, in Hz, the following expressions should be used:

Stiffness: $k' = A_1 (2 \pi f)^{B_1}$ N/m

Loss Coefficient: $\eta = A_2 (2 \pi f)^{B_2}$

Damping: $k'' = \eta k'$ N/m

Static Stiffness Results

In addition to the dynamic stiffness tests described above, the effect of a static load upon O-ring deflection has been investigated. Even under a static load the visco-elastic nature of the elastomer leads to time-dependent deflection as illustrated in Figure 31. Plotted here is the deflection, resulting from a sudden load application, as a function of time. It is apparent that the deflection continuously increases with time and doubles in the elapsed time between 3 seconds and 300 seconds. Even after 7 minutes the further deflection which occurs in the period between the 7 minutes and 8 minutes amounts to over 1 percent of the deflection at that point in time.

In order to obtain some meaningful comparison between the elastomers, the deflection six minutes after load application has been plotted against static load and the results are presented in Figure 32. These curves illustrate some softening of the O-rings as the static load is increased; for example, the six-minute deflection of a Buna-N ring under 200 Newtons is five times the six minutes deflection under 50 Newtons. It is seen that Buna-N and Viton 70, which are both 70 durometer materials, have very similar static stiffness. The curves further show that the 90 durometer Viton has close to 4 times the stiffness of the 70 durometer materials.

TABLE 6

POWER LAW COEFFICIENTS FOR EACH TEST CONDITION

Perturbation Parameter Value	Stiffness Coefficients		Loss Coefficient		Fig. No.	Comments
	A_1 N/m	B_1	A_2	B_2		
Nominal	3.764×10^5	.4005	.329	.1437	11	For tests other than Amp., Temp.
Nominal	4.520×10^5	.3747	.255	.1746	12	For Amp., Temp. Tests
Buna-N	2.237×10^6	.1519	.0606	.2326	13	
Viton-90	5.325×10^6	.2158	.2819	.0778	14	
Temp. 38°C	1.694×10^5	.4195	.1103	.2392	15	
Temp. 66°C	8.850×10^5	.1406	.0226	.3227	16	
Temp. 149°C	5.801×10^5	.1671	.0126	.2811	17	
Temp. 216°C	1.124×10^6	.0760	(.1)	(0)	18	
A = 1 mil	2.204×10^6	.1224	.3380	.1315	19	
A = 5 mils	2.137×10^6	.0243	.7057	-.0655	20	
A = 3/f mil	4.724×10^4	.4909	.0967	.1983	20	
Squeeze = 5%	1.231×10^5	.3592	.2853	.1748	21	
Squeeze = 10%	3.855×10^5	.3586	.2110	.1993	22	
Squeeze = 20%	7.298×10^5	.3326	.2030	.2000	23	
Squeeze = 30%	3.357×10^6	.2159	.3527	.1095	24	
Stretch = 0%	4.948×10^5	.3580	.2950	.1522	25	
Stretch = 10%	3.604×10^5	.3817	.2700	.1596	26	
X-Section = 1/16"	5.516×10^5	.338	.2150	.1982	27	
X-Section = 3/16"	3.106×10^5	.376	.1300	.2528	28	
Groove Width 115%	4.798×10^6	.049	.0449	.2675	29	Buna-N
Groove Width 150%	2.350×10^6	.136	.0532	.2534	30	Buna-N

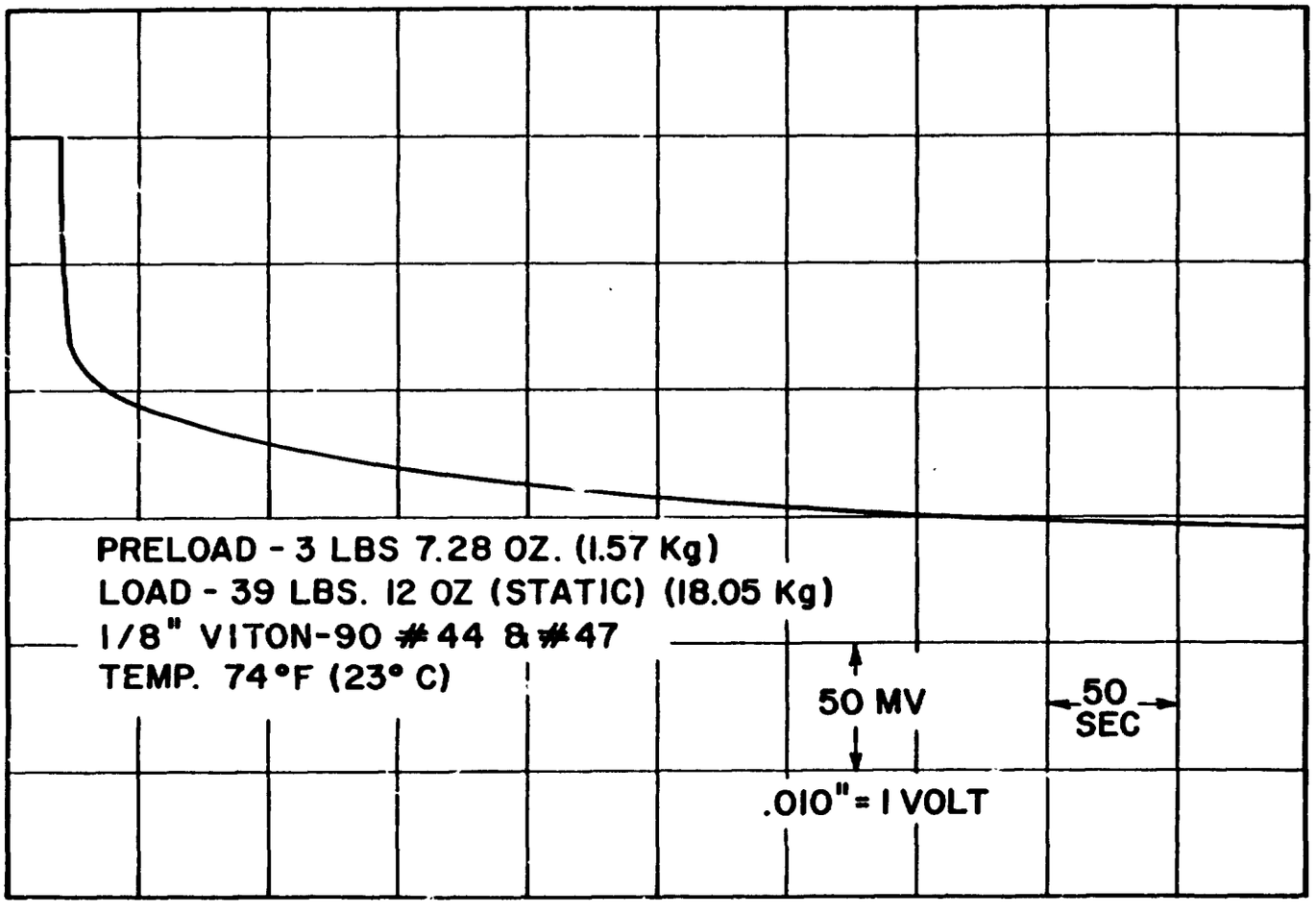

Fig. 31 Typical Trace of Deflection Versus Time under Static Load

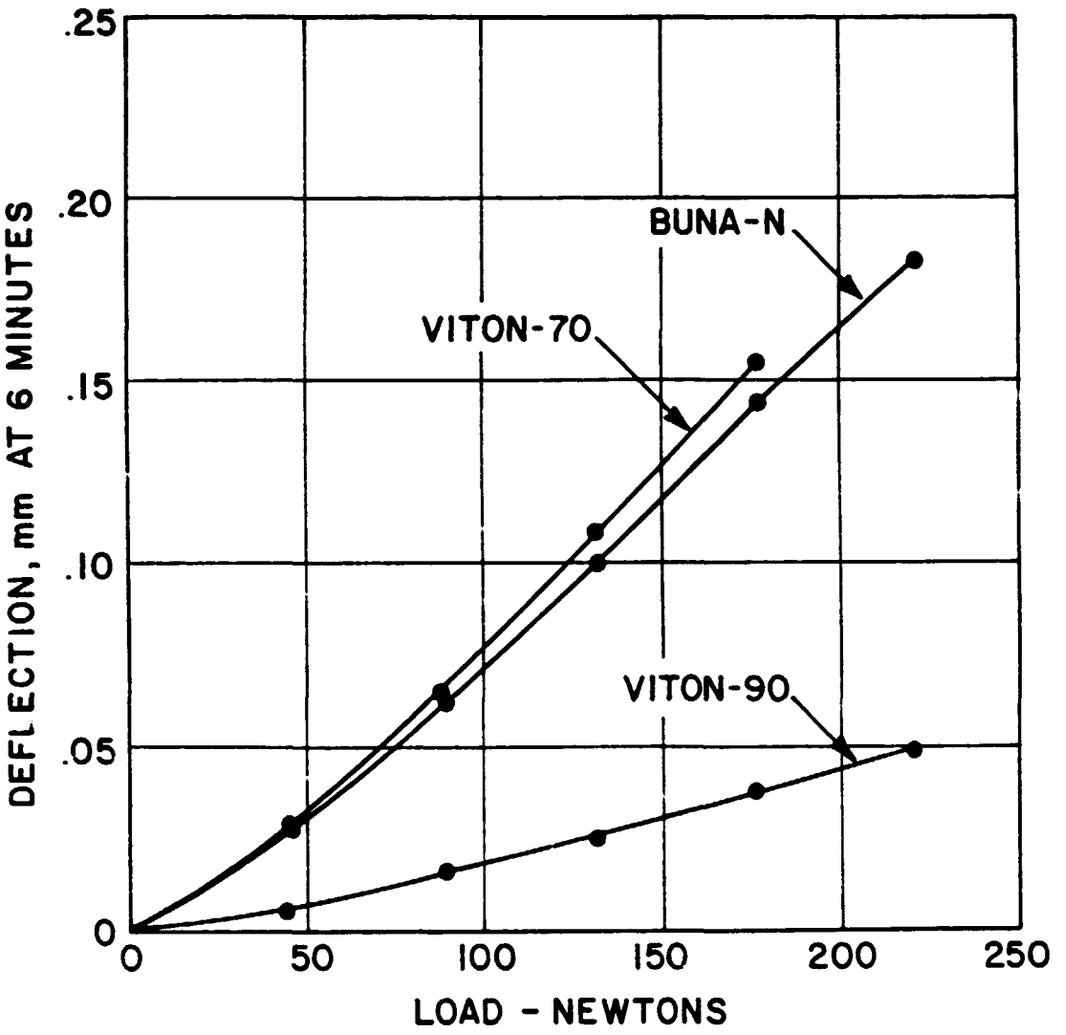

Fig. 32 "Static" Deflection as a Function of Applied Load

Table 7 provides a summary of effective static stiffness values (load/deflection) for the three materials under loads of 50, 100, and 200 Newtons. As previously discussed, the static stiffnesses are much lower than the dynamic stiffnesses. Table 8 provides the ratios of dynamic stiffness at 100 Hz and 1,000 Hz to the effective static stiffness under 200 Newtons for the three different materials and it may be seen that these ratios range from over 4 to almost 11.

TABLE 7

STATIC STIFFNESS SUMMARY

Load, Newtons	Effective Stiffness, N/m		
	Viton-70	Buna-N	Viton-90
50	1.52×10^6	1.52×10^6	7.69×10^6
100	1.29×10^6	1.38×10^6	5.71×10^6
200	1.14×10^6	1.21×10^6	4.55×10^6

TABLE 8

RATIO OF DYNAMIC STIFFNESS TO EFFECTIVE STATIC STIFFNESS UNDER 200 NEWTONS

Material	Stiffness Ratio	
	100 Hz	1000 Hz
Viton-70	4.35	10.89
Buna-N	4.91	6 98
Viton-90	4.73	7.69

4.0 DISCUSSION

It is apparent from inspection of the test data plots for individual test conditions that certain parameters have a significant effect upon O-ring dynamic characteristics and that other parameters have a less pronounced effect. To bring these trends more sharply into focus, plots have been prepared in which power law lines for each of the seven parameter perturbation ranges have, in turn, been presented on a single plot. These "trend summary" plots are presented in Figures 33 through 41 and reveal clearly the important effects of the governing parameters. The effect of all seven parameters are discussed, in turn, below.

Effects of Material

The selection of material and durometer value have a pronounced effect on the dynamic performance achieved from an O-ring flexible support, as shown in Figure 33. It may be seen that Viton-70 and Buna-N have a similar average dynamic stiffness of 6×10^6 N/m (39,000 lb/inch) but that Viton-70 has a stronger frequency dependence over the range covered, and a loss coefficient almost three times that of Buna-N. Thus, provided temperature and amplitude can be controlled, the Viton appears to be a better damping material. If higher stiffness is required, a factor of 3 to 4 increase can be achieved by a shift to 90 durometer Viton, but the loss coefficient for Viton-90 is about half that of Viton-70 and the frequency dependence of the Viton-90 properties is less pronounced than those of Viton-70.

Effects of Temperature

The effects of temperature on stiffness and loss coefficient for Viton-70 are very strong, particularly for small increases in temperature above 25 degrees Centigrade, as shown in Figure 34. Both stiffness and loss coefficients fall sharply with increasing temperature; stiffness by a factor of two or more between 25 and 66 degrees Centigrade; and loss coefficient by a factor of four. Above 66 degrees Centigrade the effects of temperature are less pronounced and no change in stiffness was observed above 149 degrees Centigrade.

The data obtained at 216 degrees Centigrade was limited due to difficulties in maintaining operation of all input and output accelerometers at this temperature. The stiffness data was very similar to that at 149 degrees Centigrade.

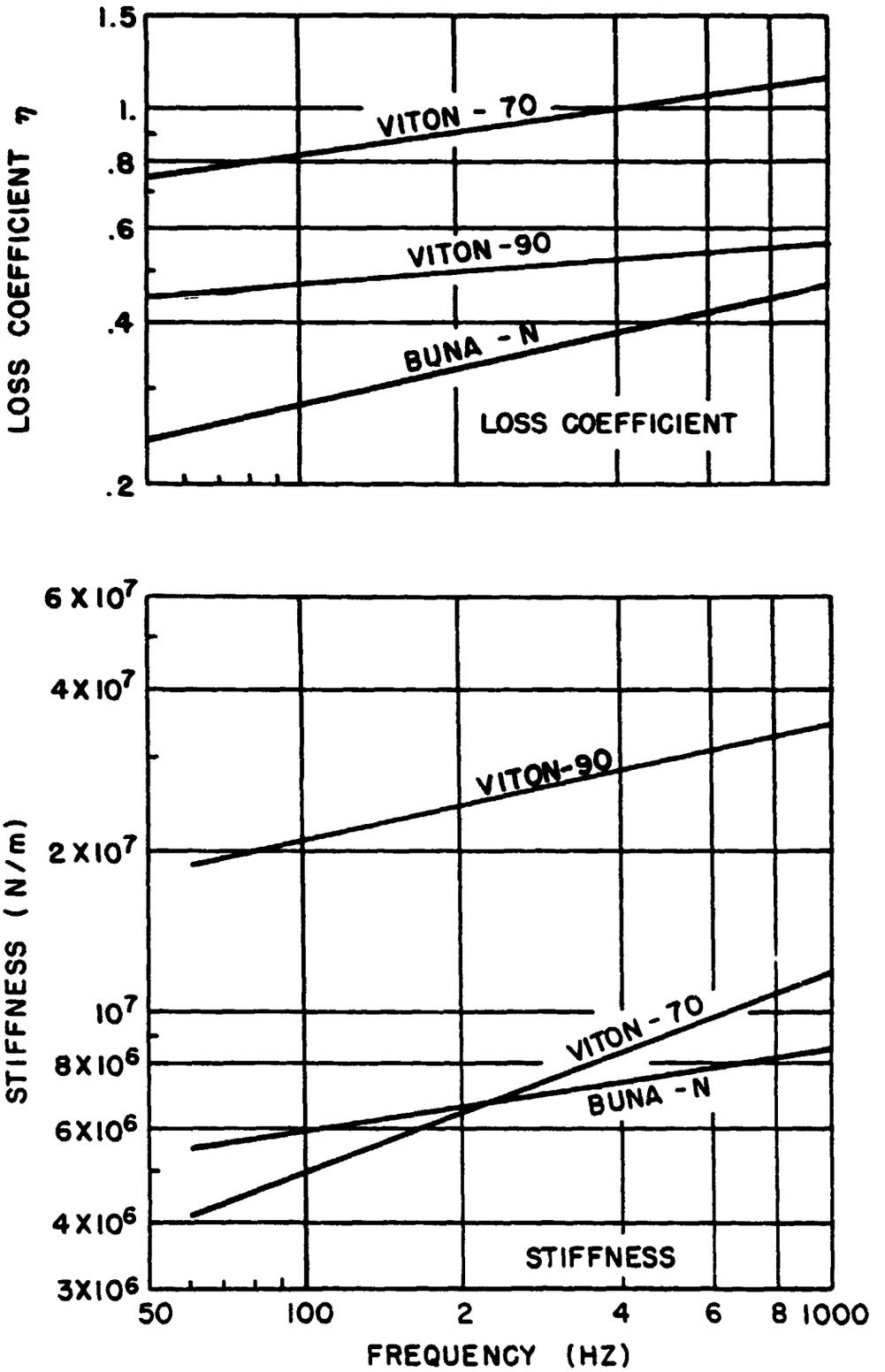

Fig. 33 Trend Summary: The Effect of Material on Stiffness and Loss Coefficient

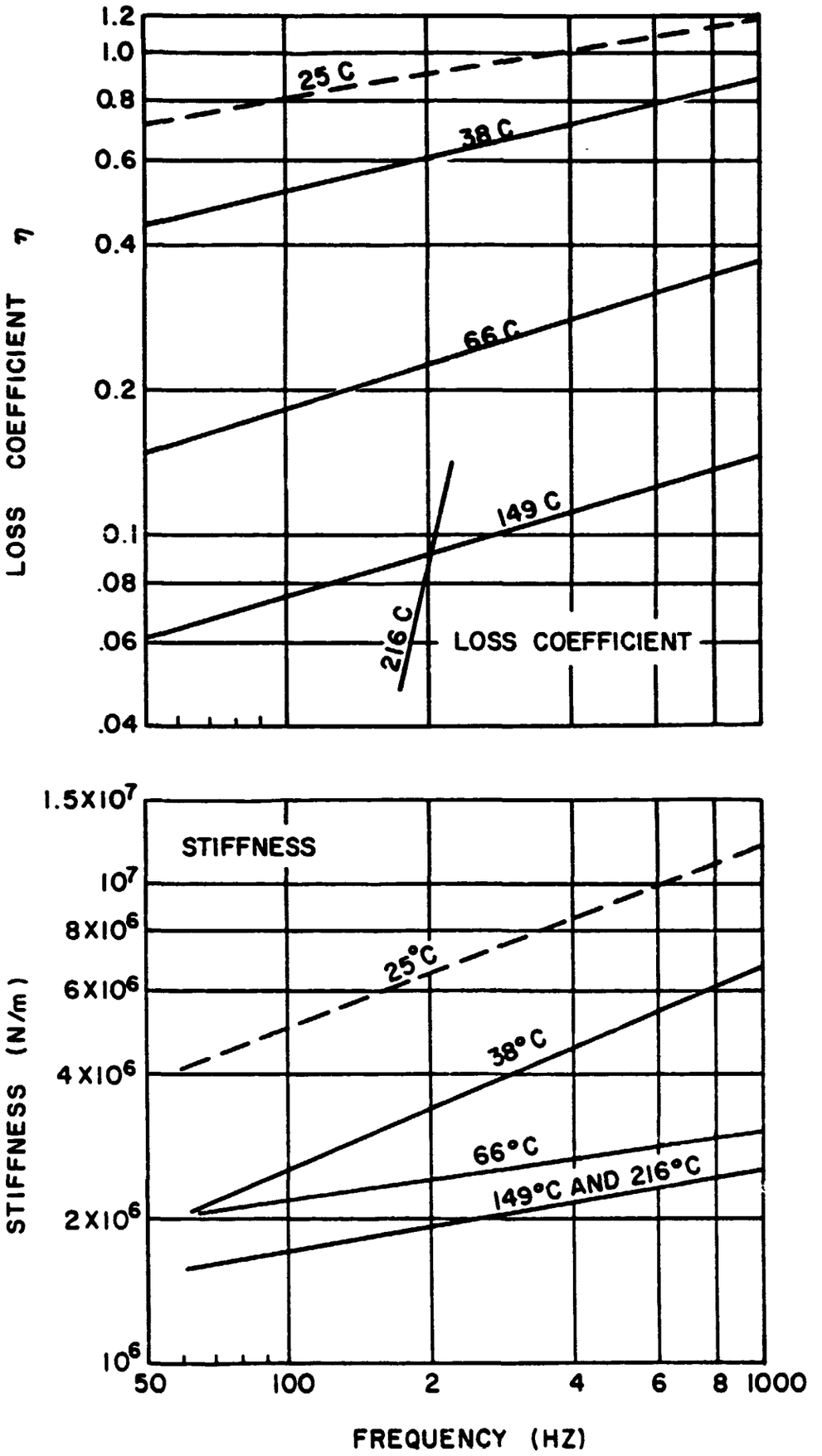

Fig. 34 Trend Summary: The Effect of Temperature on Stiffness and Loss Coefficient for Viton-70.

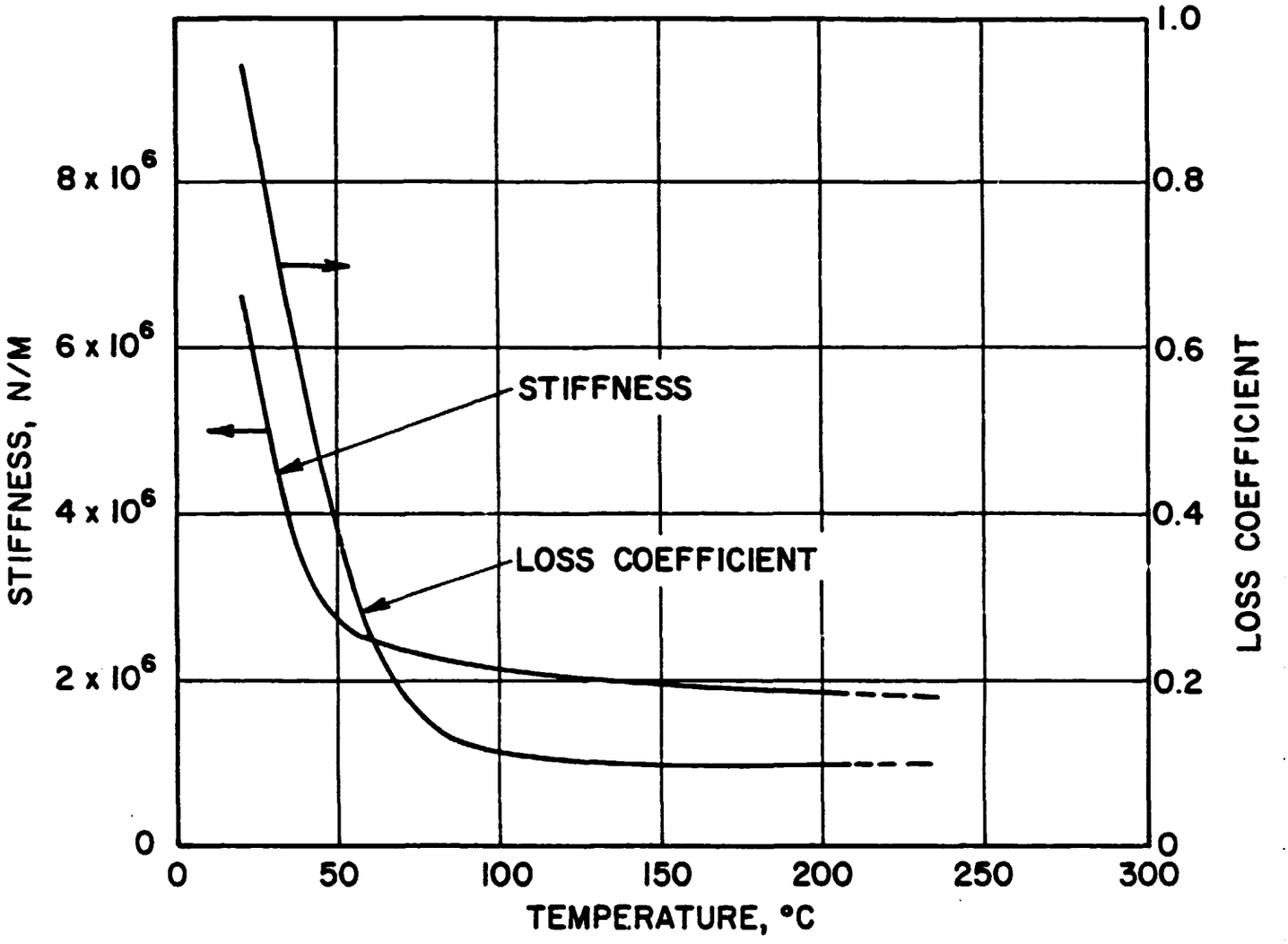

Fig. 35 Stiffness and Loss Coefficient Versus Temperature for Viton-70.

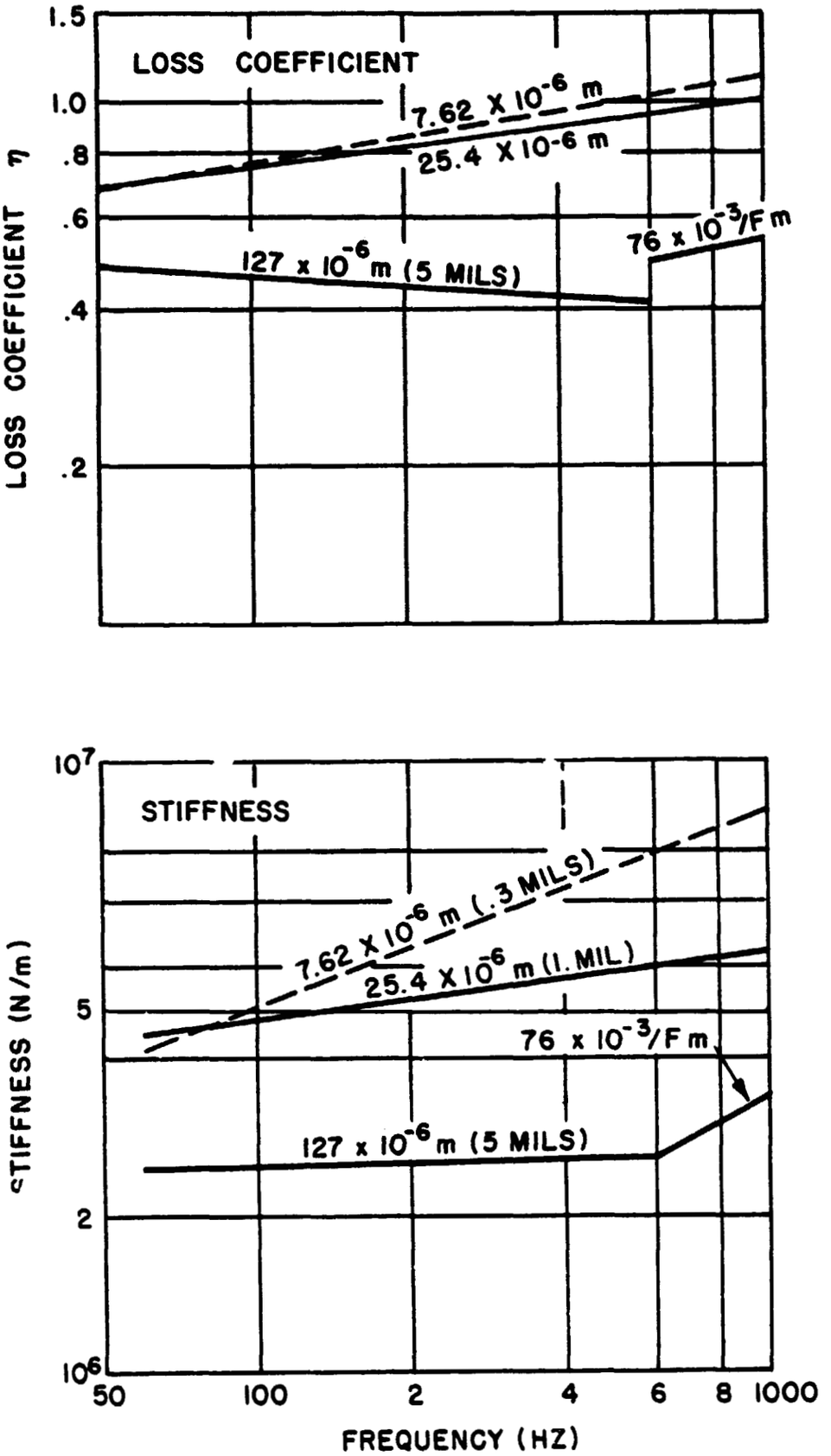

Fig. 36 Trend Summary: The Effect of Amplitude on Stiffness and Loss Coefficient for Viton-70.

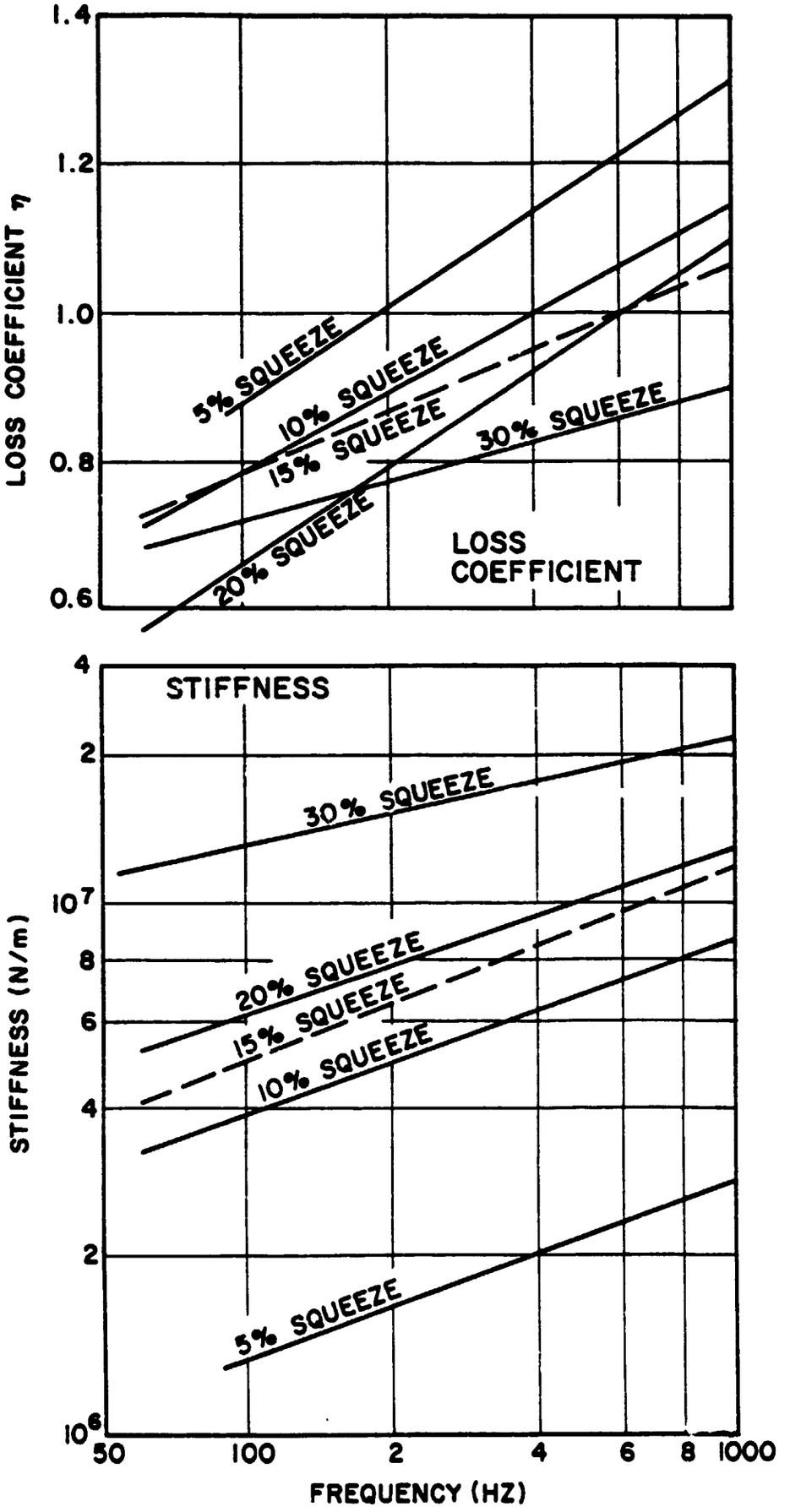

Fig. 37 Trend Summary: The Effect of Squeeze on Stiffness and Loss Coefficient for Viton-70

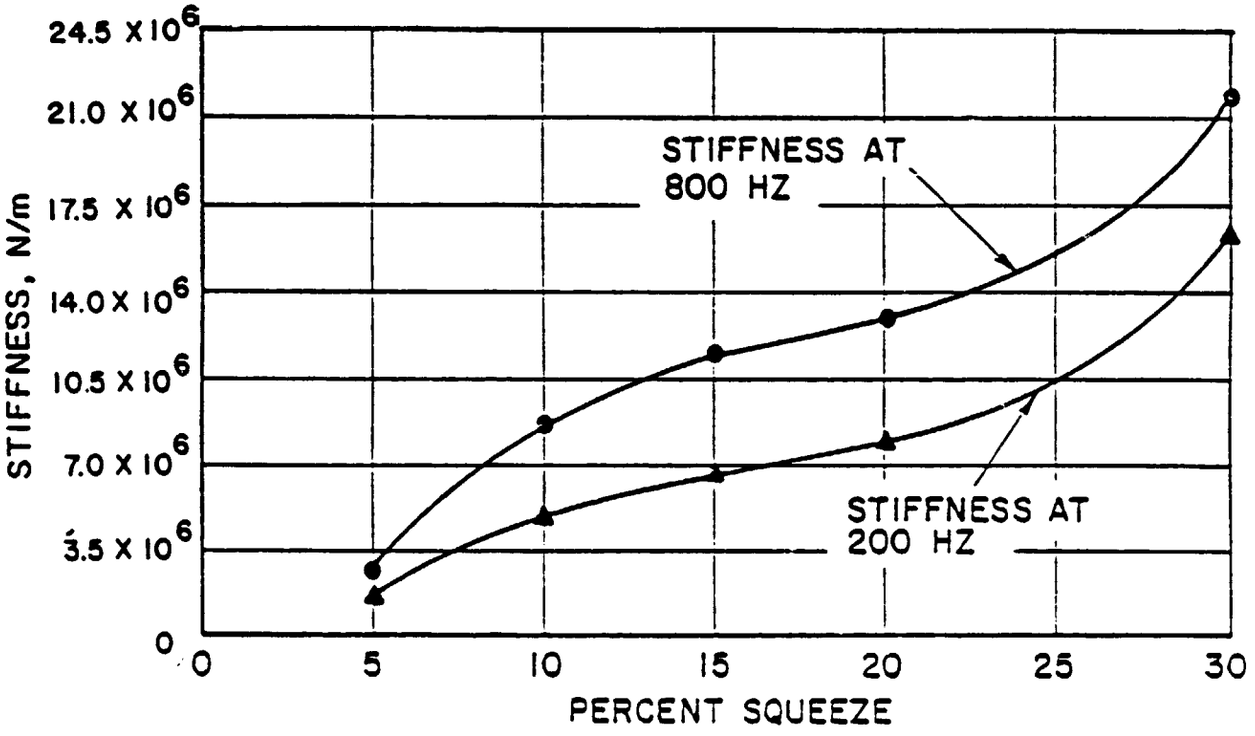

Fig. 38 Stiffness Versus Squeeze for Viton-70

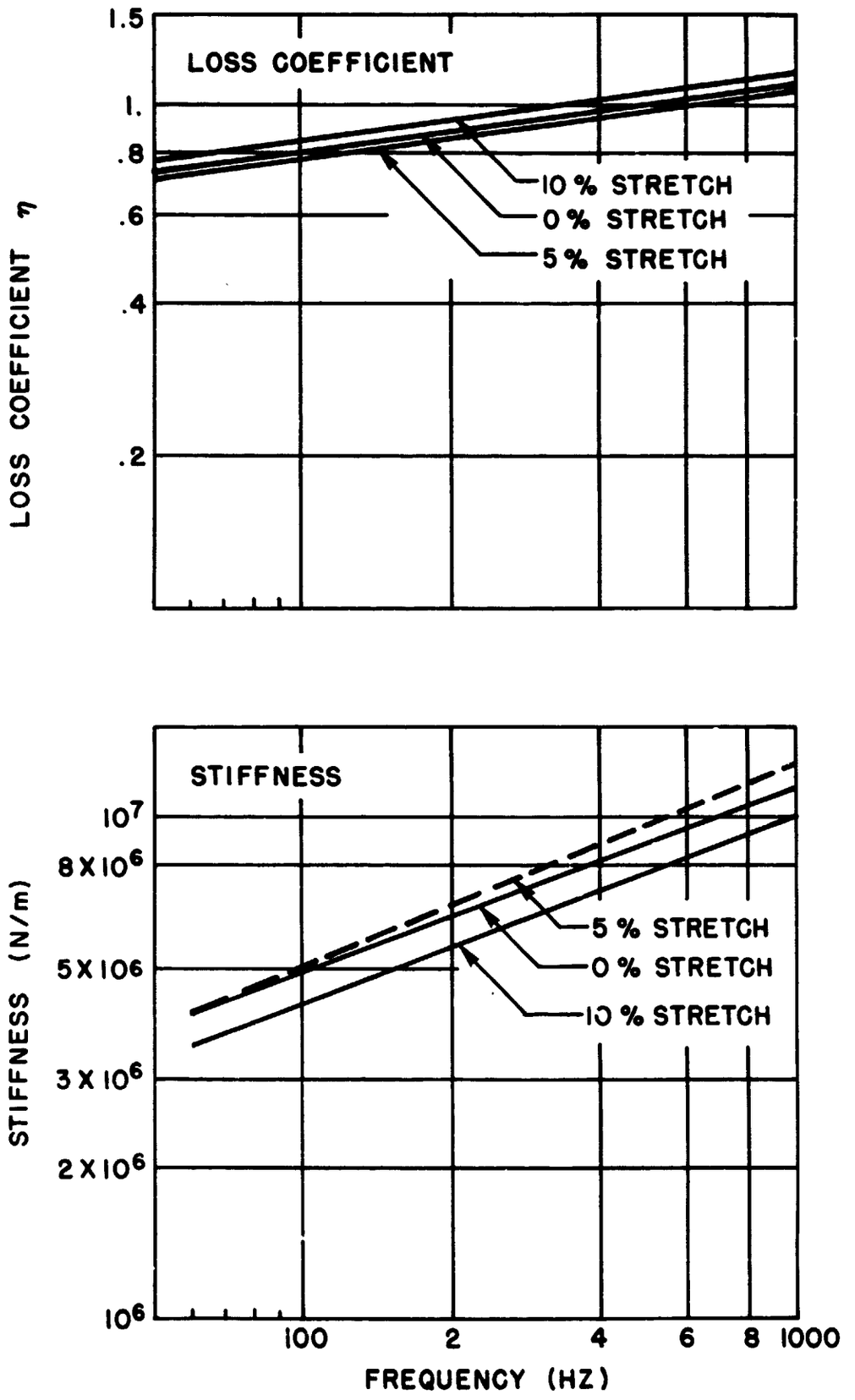

Fig. 39 Trend Summary: The Effect of Stretch on Stiffness and Loss Coefficient for Viton-70.

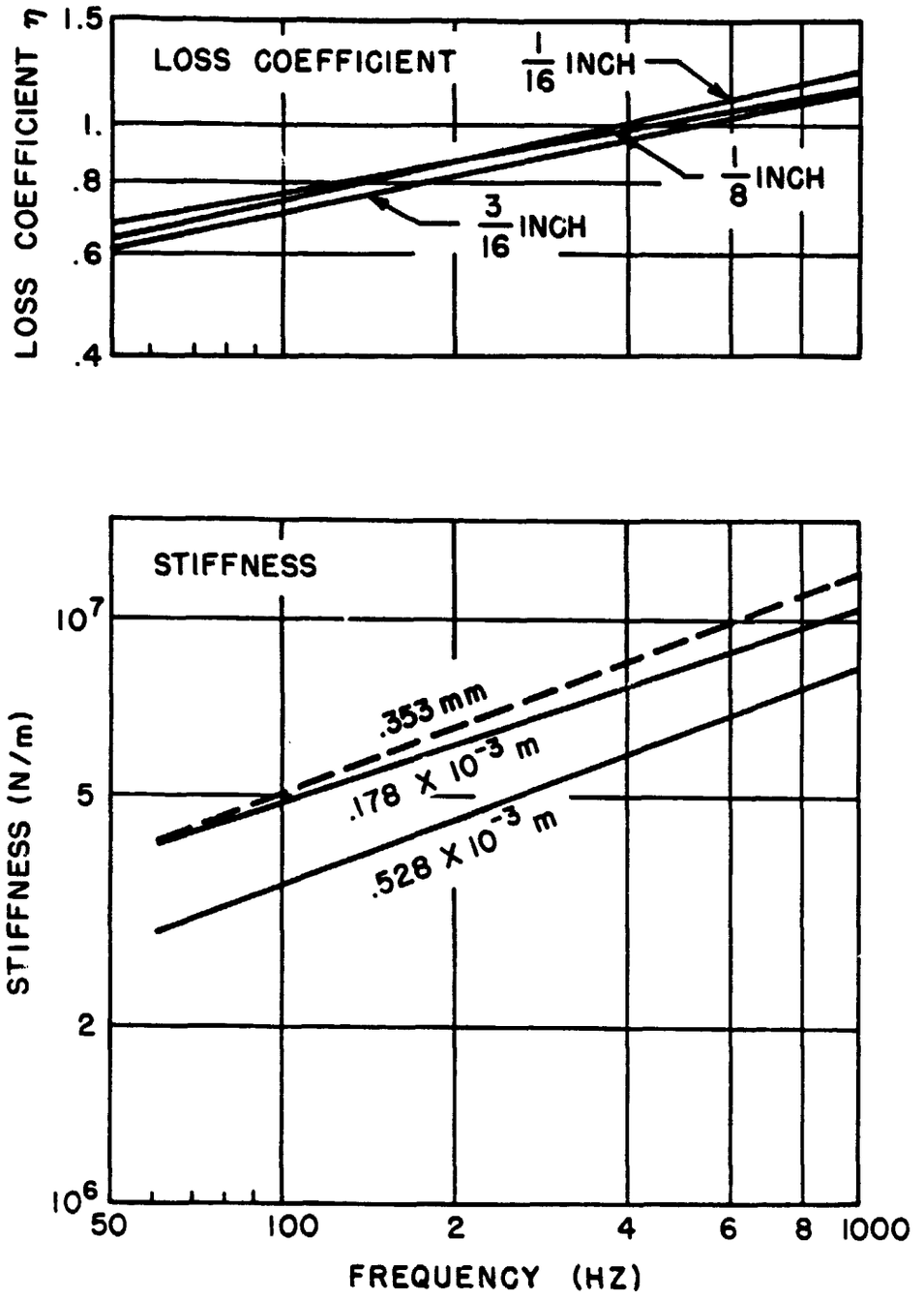

Fig. 40 Trend Summary: The Effect of Cross-Section Diameter on Stiffness and Loss Coefficient for Viton-70.

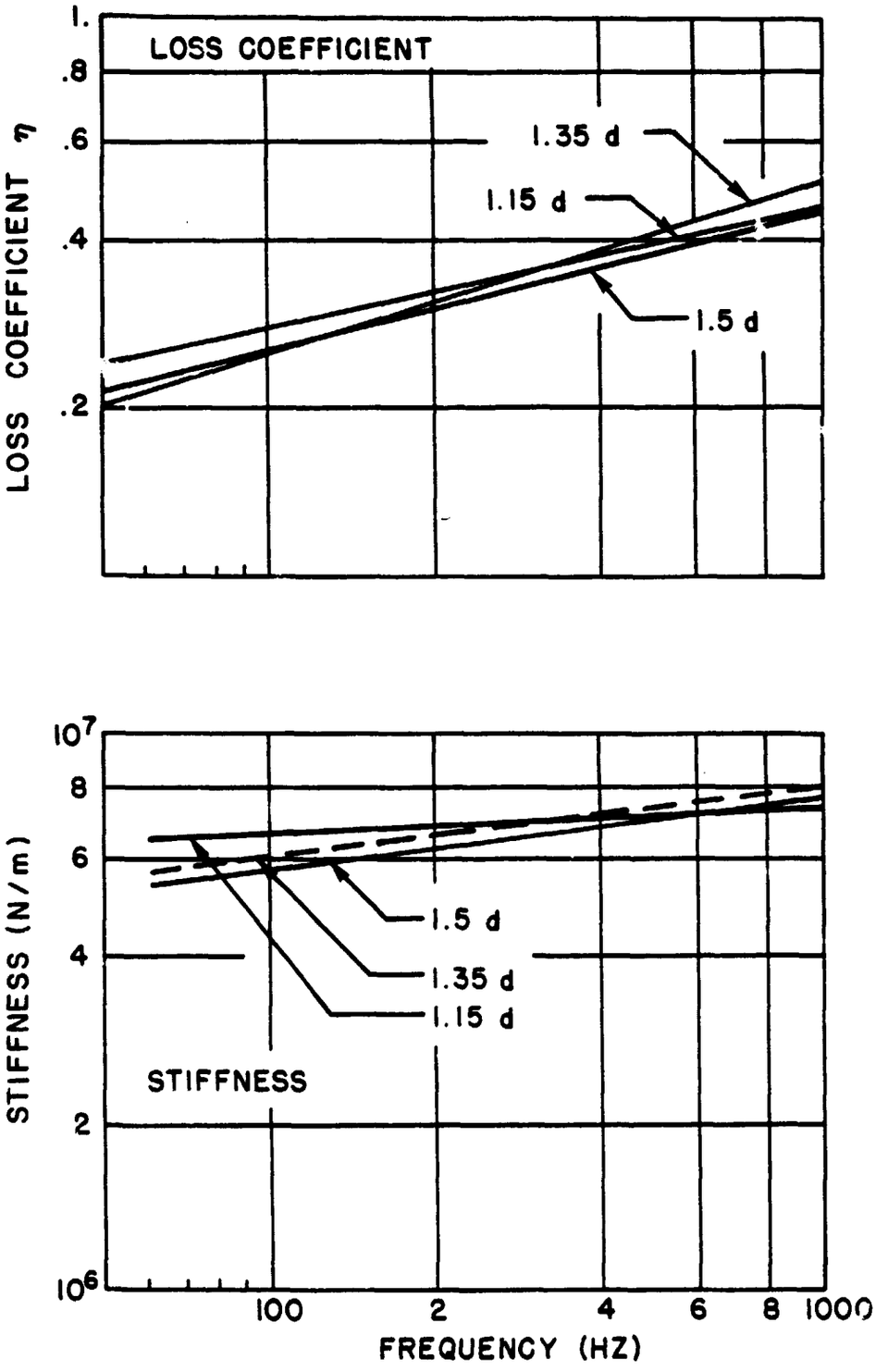

Fig. 41 Trend Summary: The Effect of Grocve Width on Stiffness and Loss Coefficient for Buna-N.

The loss coefficient data presented the trend shown in Figure 18 over the frequency range 170 to 220 Hz and it is suspected that the suggestion of sharply changing loss coefficient was actually experimental scatter rather than a true trend. The trends in stiffness and loss coefficient as a function of temperature are emphasized by a cross-plot of these quantities vs. temperature, at 200 and 800 Hz (Figure 35).

In summary, the behavior of Viton-70 with changing temperatures indicates that, while it can survive high temperatures, this material does not retain the high damping properties observed at room temperature.

Effects of Amplitude

The effect of amplitude on stiffness and loss coefficient is strong, as shown in Figure 36. In the range 100 Hz to 1000 Hz increasing amplitude consistently decreases stiffness and damping, and decreases their frequency dependence. At 500 Hz even a modest increase in amplitude from 7.62×10^{-6} m (0.3 mil) to 25.4 10^{-6} m (1 mil) cuts the stiffness by over 30 percent and an increase to 127×10^{-6}m (5 mils) causes an additional reduction of over 50 percent. Loss coefficient is less strongly affected, an increase from 7.67×10^{6} m to 127×10^{-6} m cutting loss coefficient from 1 to 0.43. Intuition suggests that self-heating of the elastomer is a contributory cause of the stiffness degradation; 3.8 watts/cm^3 were being dissipated at 500 Hz and 127×10^{-6} m amplitude and it was necessary to blow cold air on the test specimen to hold the surrounding metal temperatures at its desired reference value. At the same time, results of Reference 3 suggest that the influence of dynamic strain on elastomer material behavior is a contributor to stiffness degradation. This question of the relative importance of strain and self-heating cannot be resolved without a detailed thermal analysis and. possibly, additional temperature measurements. For design purposes, it is primarily important that account be taken of this measured stiffness degradation in dynamic analysis of systems using elastomer O-rings to dissipate vibration energy.

Effects of Squeeze

The radial precompression, or squeeze, imposed on the O-ring will affect its dynamic behavior, particularly its stiffness, as shown in Figure 37. The

primary reason is the hertzian nature of the contact - increasing squeeze increases the area of contact between the ring and metal, and, thereby, the force which can be developed for a given relative radial displacement. For squeeze values in the region of 15 percent (see Figure 10 for definition of squeeze), the stiffness is least sensitive to squeeze, which probably makes 15 percent a good design value of squeeze. As squeeze is dropped to 5 percent, the stiffness starts to fall off sharply; a contributory reason is that under even light gravity loads, contact between ring and metal is not maintained over 360° when 5 percent squeeze is coupled with the reference value of 5 percent stretch. The interaction of squeeze and stretch must be recognized in that, when the ring is stretched, its effective cross-sectional diameter is reduced and the effective squeeze is less than the squeeze as defined in Figure 10.

When squeeze is increased to 30 percent, stiffness increases more rapidly than at 15 percent. The reason could be contact between groove walls and ring or simply the increased rectangularity of the squeezed O-ring cross-section and an increased influence of elastomer bulk modulus on deflection characteristics. The trends in stiffness as a function of squeeze are emphasized in Figure 38, which is a cross-plot of stiffness versus squeeze at 200 Hz. It shows the turning point at around 15 percent squeeze.

The influence of squeeze on loss coefficient is less pronounced than on stiffness, but the general tendency is for increasing squeeze to reduce the loss coefficient. Between a squeeze of 5 percent and a squeeze of 30 percent, the loss coefficient drops by approximately 0.25 for Viton-70.

In summary, 15 percent is a good value to select for squeeze unless special requirements dictate otherwise.

Effects of Stretch

The influence of stretch on stiffness and loss coefficient is shown in Figure 39. It is apparent that no clear trend can be defined since 5 percent stretch causes a higher stiffness and lower loss coefficient than either 0 or 10 percent, and secondly because the spread for all stretch values is only 20 percent in stiffness and 10 percent in loss coefficient.

Stretch is, therefore, shown to be of little direct importance, and there is no clear motivation for the designer to select any other value than 5 percent.

Effects of Cross-Sectional Diameters

As shown in Figure 40 cross-sectional diameter is another parameter which develops no clear trend within the available test results. The reference value of 1/8 for cross-section diameter develops the highest stiffness and either a smaller or larger cross-section causes a reduced stiffness. For loss coefficient the spread of values is very small and some intersection of the lines occurs.

Simple analysis would suggest that cross-sectional diameter should have little effect provided squeeze remains the same; both stressed and strained dimensions of the cross-section are proportional to cross-section diameter and stiffness should, therefore, be independent of this diameter. Secondary effects such as stretch-squeeze interaction and the dependence of strain on diameter for constant amplitude may cause some secondary trends, which could only be clearly identified by more extensive testing.

Effects of Groove Width

As would be expected, groove width has a negligible effect on stiffness and loss coefficient. This statement would have to be modified only if interaction of an O-ring with the groove walls occurred. Since the smallest groove width investigated was 1.15 times the cross-sectional diameter, this interaction did not occur and, as shown in Figure 41, very similar stiffness and loss coefficient values were obtained for all three groove widths considered.

The most notable feature of Figure 41 is that the stiffness and loss coefficient do not correspond to the reference values for other tests. This is because, inadvertantly, a Buna-N O-ring was used for these tests instead of a Viton-70 ring. The conclusion of a negligible effect of groove width is expected to be the same for Viton-70.

The recommended value for groove width (from O-ring design guides) is 1.35d and this is shown to be an entirely satisfactory value to use. If space is at a premium, 1.15 is also an acceptable value from dynamic performance considerations.

In summary, the results presented in this report effectively identify important parameters in determining stiffness and damping of flexible bearing mounts in the form of O-rings. It is pointed out, however, that the work is totally empirical, applied to idealized components, and involves perturbations in individual test parameters. In addition, the data was obtained with new O-rings in a dry environment. In order to continue the learning process which this investigation has started, the following further investigations are considered important.

1. Determination of interaction between material, temperature, amplitude, and squeeze, including coverage of a wider range of materials.
2. Determination of the effect of an oily environment on dynamic characteristics.
3. Determination of long-term effects of both static and dynamic load upon dynamic stiffness and damping.
4. Development of empirical relationships between the material shear moduli and specimen stiffness and loss coefficient.
5. Development of analytical predictions of O-ring stiffness.
6. Applications analysis to assess the viability of dampers with component stiffness and damping values exhibited by those O-rings tested in the present investigation.
7. Application testing of an elastomeric O-ring damper.

The last two items are of near-term importance since they would provide demonstration of the technology already developed. Item 7 would identify any other pertinent parameters which are not apparent from component test results obtained thus far. With reference to Item 1 of this list, a tractable investigation to reveal combined effect of the four major parameters can be contemplated since the parameters of less importance may be eliminated. A wider range of material to include Neoprene, Urethane, and Fluoro-silicone as a minimum is desirable. With reference to Item 2, it is to be expected that oil would have some influence on the static and dynamic contact conditions between elastomer and metal. With reference to Item 3, it is essential that the potential for deterioration and change in performance with time under load be identified before routine design

of these components can be contemplated for long-life applications. With reference to Items 4 and 5, it is clearly desirable that relationships between material properties and component properties be established to allow application of O-rings of other materials.

5.0 CONCLUSIONS

1. O-ring dynamic stiffnesses in the range of 100 to 1,000 Hz are between 4 and 11 times measured static stiffnesses.
2. Material and radial squeeze are the parameters which offer the designer most direct control over the dynamic characteristics of an O-ring.
3. Pronounced trends have not been observed in the effect of stretch, cross-sectional diameter, and groove width on O-ring dynamic characteristics.
4. Temperature and vibration amplitude have a strong effect on O-ring dynamic characteristics and must be carefully accounted for in designing for particular applications.
5. The high loss coefficient of Viton-70 O-rings at room temperature falls off noticeably as the temperature is increased. Stiffness follows a similar trend.
6. Increasing amplitude decreases the effective stiffness and loss coefficient of Viton-70 O-rings.

6.0 RECOMMENDATIONS

The basic investigation presented in this report should be expanded in the following ways:

1. Applications analysis and testing.
2. Determination of interaction between material temperature, amplitude, and squeeze, including tests of a wider range of materials.
3. Determination of the effects of an oily environment.
4. Determination of long-term static and dynamic loading effects upon the dynamic characteristics of O-rings.
5. Development of empirical relationships between the material shear moduli and specimen stiffness and loss coefficient.
6. Development of analytical predictions of O-ring stiffness and damping.

REFERENCES

1. Chiang, T., Tessarzik, J.M., and Badgley, R.H., Development of Procedures for Calculating Stiffness and Damping Properties of Elastomers in Engineering Applications, Part I: Verification of Basic Methods, NASA Report CR120905, March 1972. Prepared by MTI for NASA-Lewis Research Center under Contract NAS3-15334.

2. Gupta, P.K, Tessarzik, J.M., and Cziglenyi, L., Development of Procedures for Calculating Stiffness and Damping Properties of Elastomers in Engineering Applications, Part II: Elastomer Characteristics at Constant Temperature, NASA Report CR-134704, prepared by MTI for NASA-Lewis Research Center under Contract NAS3-15334, April, 1974.

3. Smalley, A.J., and Tessarzik, J.M., Development of Procedures for Calculating Stiffness and Damping Properties of Elastomers in Engineering Applications, Part III: The Effects of Temperature, Dissipation Level and Geometry, NASA Report CR-134939, prepared by MTI for NASA-Lewis Research Center under Contract NAS3-15234, and Contract NAS3-18546, November, 1975.

4. Smalley, A.J., Tessarzik, J.M., and Badgley, R.H., "Testing for Material Dynamic Properties", ASME Publication: Vibration Testing - Instrumentation and Data Analysis, AMD-Vol. 12, 1975, p. 117.

5. Snowden, J.C., "Vibration and Shock in Damped Mechanical Systems", John Wiley and Sons, Inc., New York, New York.

6. Harris, C.M., and Crede, C., "Shock and Vibration Handbook", McGraw-Hill, New York, 1961.